

WORKSHOP:

FROM BASIC TO APPLIED RESEARCH TOWARDS DURABLE AND RELIABLE FUEL CELLS

Lucerne, Switzerland, 5 July 2022

Online THDA for rSOC diagnostic: Illustration for reactants depletion

G. Hammerschmid^{1,2}, H. Moussaoui^{1*}, J. Van herle¹, V. Subotić²

hamza.moussaoui@epfl.ch



¹Group of Energy Materials, École Polytechnique Fédérale de Lausanne, Switzerland



²Institute of Thermal Engineering, Graz University of Technology, Austria

Contents

1. Introduction
2. Experimental Method
3. Modeling
4. Experimental Results
5. Model Validation and Results
6. Conclusion

Context

Introduction

Exp. method

Modeling

Exp. results

Model results

Conclusion

Main limitation of solid oxide cells:

- Durability insufficient for large-scale deployment
- Critical conditions cause premature failure or irreversible degradation

Solution:

- Early detection & identification of critical cond.
- Mitigation and recovery
- No irreversible degradation

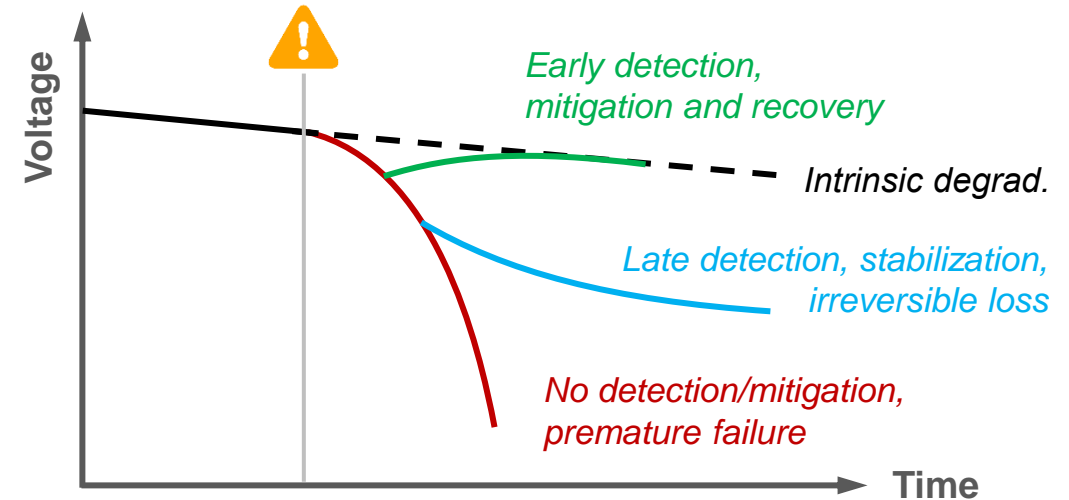


Fig.1: Voltage evolution and possible degradation pathways under failure.

SCOPE

Experimental investigation of fuel and steam starvation:

- Polarization curves (jV)
- Electrochemical Impedance Spectroscopy (EIS) and Distribution of Relaxation Times (DRT)
- Total Harmonic Distortion (THD)

2D, steady-state **simulation model** with MATLAB

Electrochemical Impedance Spectroscopy (EIS)

- Introduction
- Exp. method
- Modeling
- Exp. results
- Model results
- Conclusion

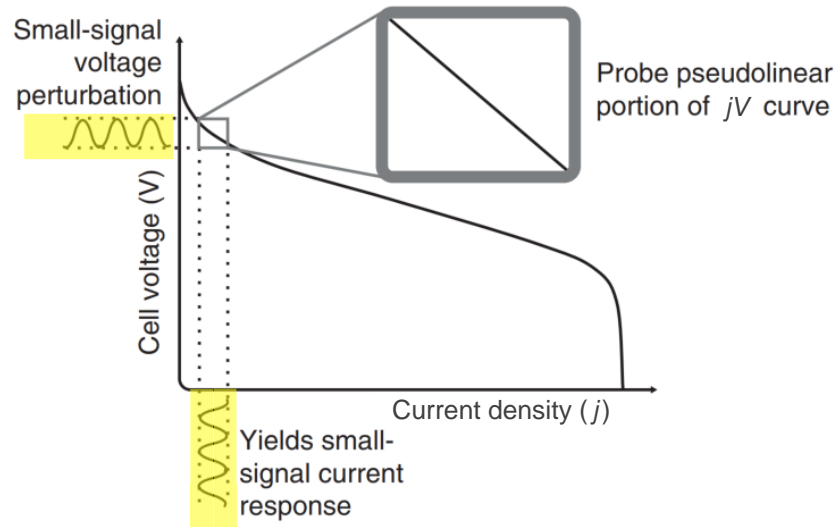


Fig.2: EIS method from "Fuel Cell Fundamentals" (O'Hayre et al., 2016).

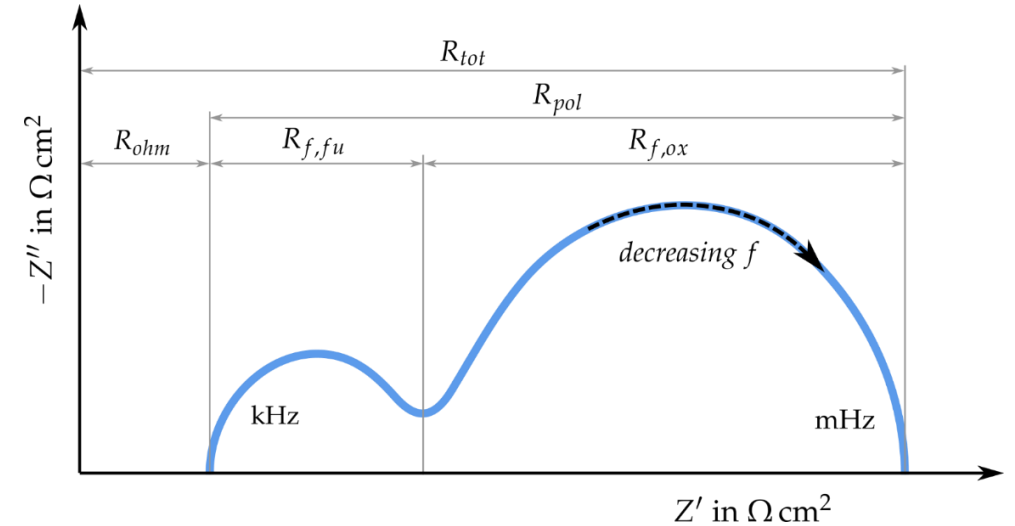


Fig.3: Schematical representation of an impedance spectrum as Nyquist plot.

Impedance:
$$Z(\omega) = \frac{U(t)}{j(t)} = \frac{\hat{U} \sin(\omega t + \phi)}{\hat{j} \sin(\omega t)} = \frac{\hat{U} e^{i(\omega t + \phi)}}{\hat{j} e^{i\omega t}} = \hat{Z} e^{i\phi} = \hat{Z} (\cos \phi + i \sin \phi) \quad \text{Eq. (1)}$$

DRT (Distribution of Relaxation Times):

$$Z_{\text{DRT}}(\omega) = R_{ohm} + \int_{-\infty}^{\infty} \frac{\gamma(\ln \tau)}{1 + i\omega\tau} d(\ln \tau) \quad \text{Eq. (2)}$$

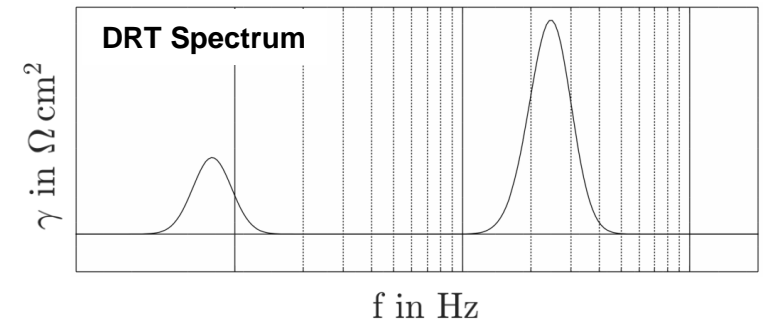
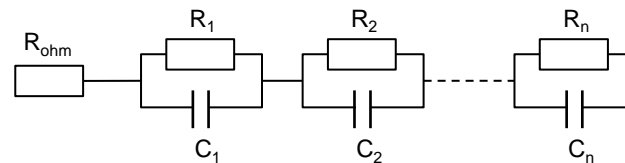
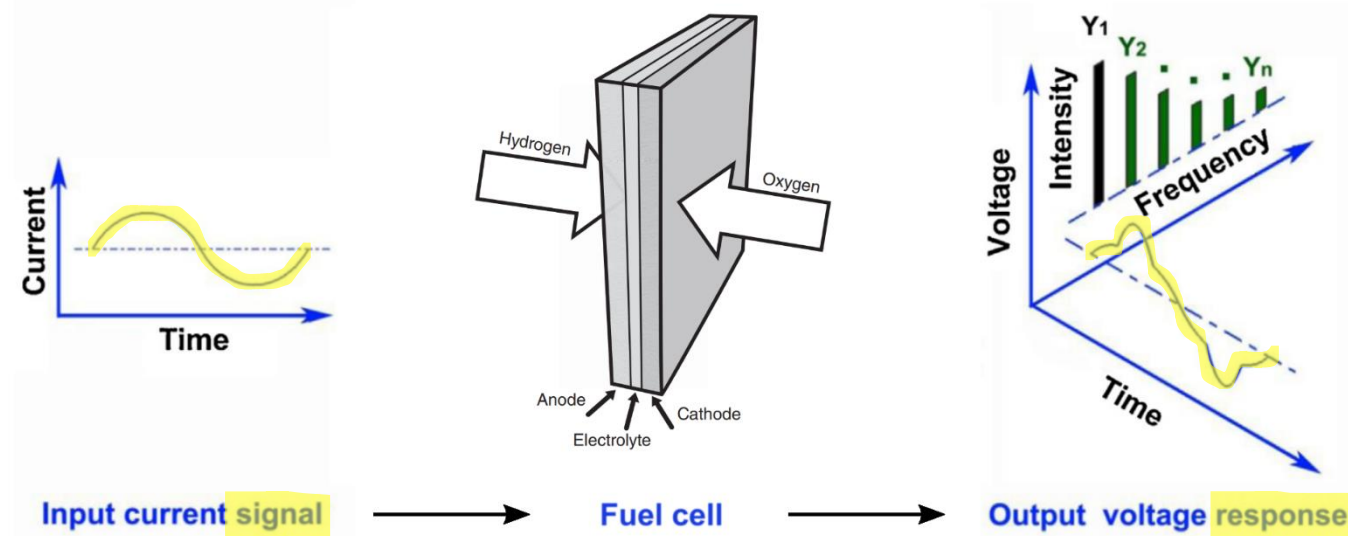


Fig.4: Schematical representation of a DRT spectrum.

❖ Well established but still a **laboratory tool** (sophisticated to implement in a commercial context)

Total Harmonic Distortion (THD)

- Introduction
- Exp. method
- Modeling
- Exp. results
- Model results
- Conclusion



$$\text{THD} = \frac{\sqrt{\sum_{n=2}^{\infty} Y_n^2}}{Y_1} \quad \text{Eq. (1)}$$

Y_1 amplitude of fundamental frequency
 (= frequency of excitation signal)
 $Y_2 \dots Y_n$ amplitudes of higher harmonics

Fig.5: Schematic voltage response to a sinusoidal current signal in time and frequency domain from "Total harmonic distortion analysis of oxygen reduction reaction in proton exchange membrane fuel cells" (Mao and Krewer, 2013).

- Quantifies the **non-linearity** (no sinusoidal response)
- Deconvolution of response into **harmonics** (via Fourier transform)
- **Hypothesis:** Identification of critical conditions via frequency-specific distortion (compared to healthy, linear state)
- At const. operation, **THD index** dependent on:
 - f_1 frequency of excitation signal
 - j_{AC}, U_{AC} amplitude of excitation signal
 - n number of harmonics used

Single Cell Setup and Test Rig

- Introduction
- Exp. method
- Modeling
- Exp. results
- Model results
- Conclusion

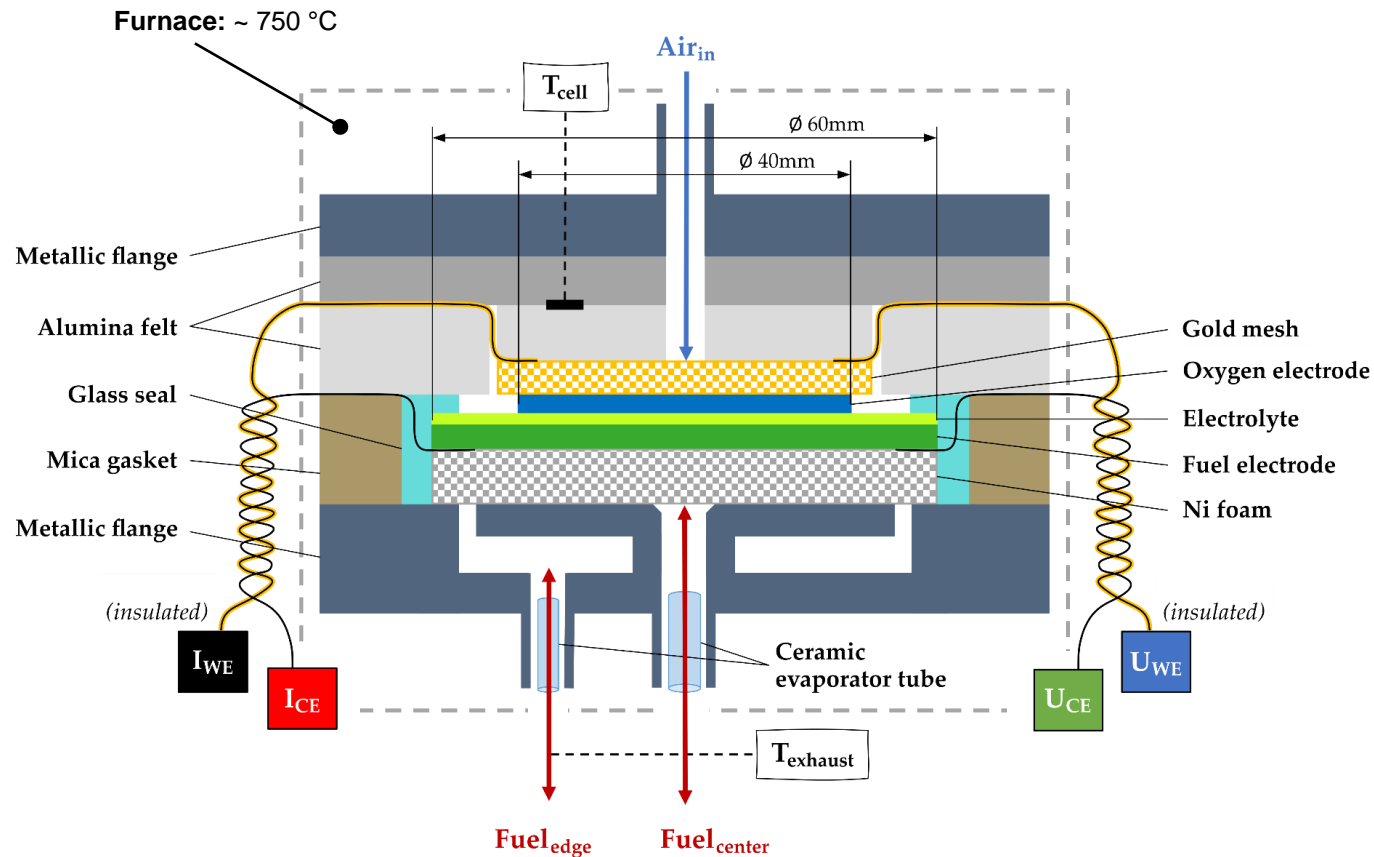


Fig.6: Schematic representation of the single cell setup.

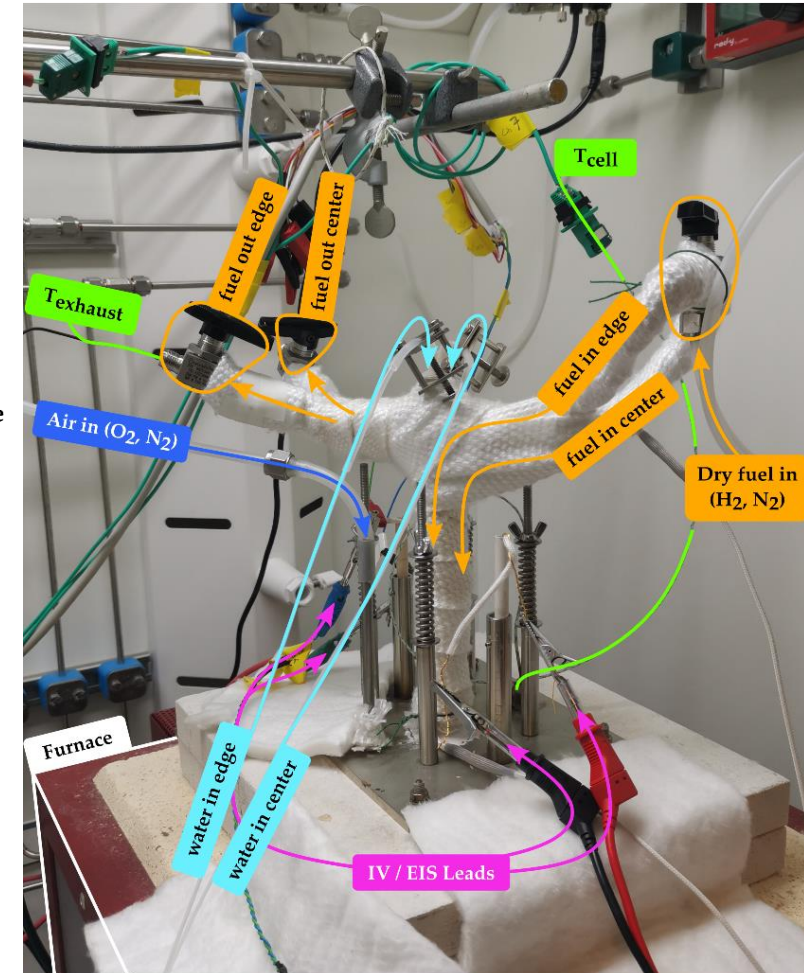


Fig.7: Photo of the experimental test rig.

- Introduction
- Exp. method
- Modeling**
- Exp. results
- Model results
- Conclusion

Modeling

Fitted to experimental data

Nernst: but considering parasitic losses j_{leak} $\rightarrow p_{i,in}^e$

$$OCV = -\frac{\Delta_r G(T, p^\theta)}{z_e F} - \frac{RT}{z_e F} \ln \left(\prod_i \left(\frac{p_{i,in}^e}{p^\theta} \right)^{v_{st,i}} \right) \quad \text{Eq. (3)}$$

Charge transfer: Butler-Volmer

$$j = j_0 \left\{ \exp \left(\frac{\alpha z_e F \eta_{act}}{RT} \right) - \exp \left(-\frac{(1-\alpha) z_e F \eta_{act}}{RT} \right) \right\} \quad \text{Eq. (4)}$$

$$j_0 = \gamma_0 \exp \left(-\frac{E_{a,0}}{RT} \right) \quad \text{Eq. (5)}$$

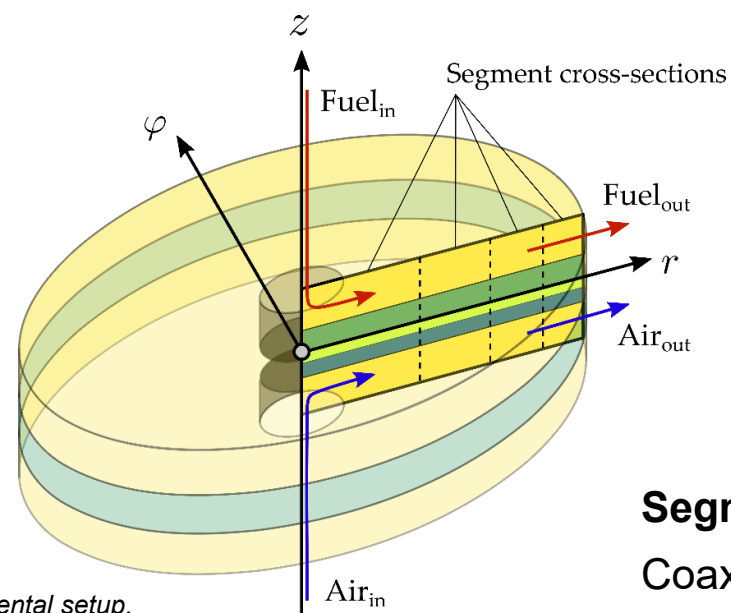
Charge transport: Ohm's law

$$\eta_{ohm} = j R_{ohm} = j R_{ohm,0} \exp \left(\frac{E_{a,ohm}}{RT} \right) \quad \text{Eq. (6)}$$

Change in electrochemical potential:

$$\eta_{conc} = \frac{RT}{z_e F} \ln \left(\prod_i \left(\frac{c_{i,j \neq 0}}{c_{i,j = 0}} \right)^{v_{st,i}} \right) \quad \text{Eq. (7)}$$

jV Model: $U(j) = OCV - \eta_{act} - \eta_{ohm} - \eta_{conc}$ Eq. (2)



Segmentation:
Coaxial cylinders with equal active area

→ Correction factor C for η_{conc}

Fig. 8: Computational domain based on the experimental setup.

Fuel Starvation (SOFC)

- Introduction
- Exp. method
- Modeling
- Exp. results**
- Model results
- Conclusion

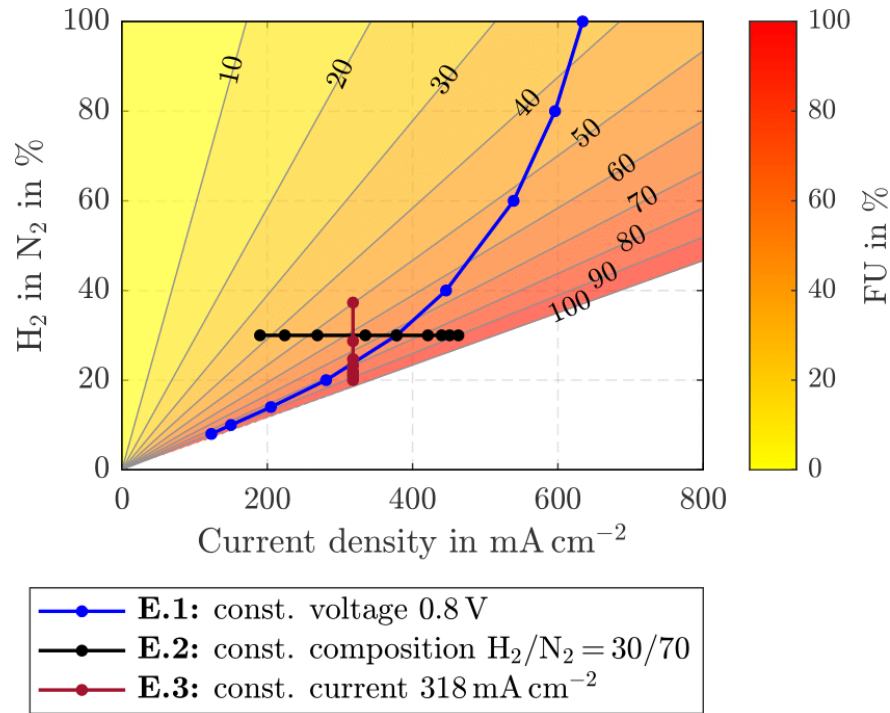


Fig.9: FU with current density and composition (150 Nml min⁻¹, 12.57 cm²).

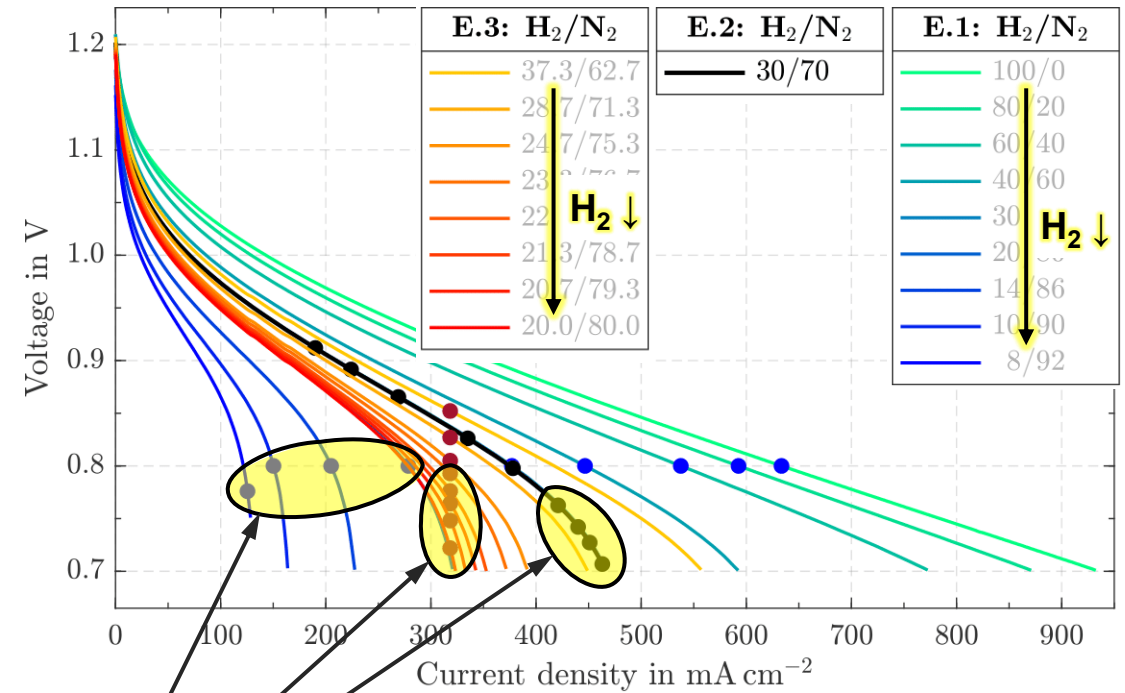


Fig.10: jv curves of fuel starvation. The dots indicate operating points of EIS and THD measurements.

Fuel Utilization:
$$FU = \frac{jA_{cell}}{z_e F \dot{n}_{H_2}} \quad \text{Eq. (8)}$$

- For **FU > 80%** significant voltage drop (↑ η_{conc})

Fuel Starvation (SOFC)

- Introduction
- Exp. method
- Modeling
- Exp. results**
- Model results
- Conclusion

	No	E.3)	E.1)	E.2)
		FU %	FU %	FU %
1		50	37	37
2		65	43	43
3		75	52	52
4		80	65	65
5		84	74	74
6		87	82	82
7		90	86	86
8		93	88	88
9			90	90

$H_2 / N_2 =$ **20.7 / 79.3** **8 / 92** **30 / 70**

- R_{ohm} and high-frequency semicircle $\neq f(FU)$
- R_{pol} and low-frequency semicircle $\uparrow\uparrow$ as $FU \uparrow$
- For same FU , impedance \uparrow for diluted fuel and low j than for H_2 rich fuel and high j

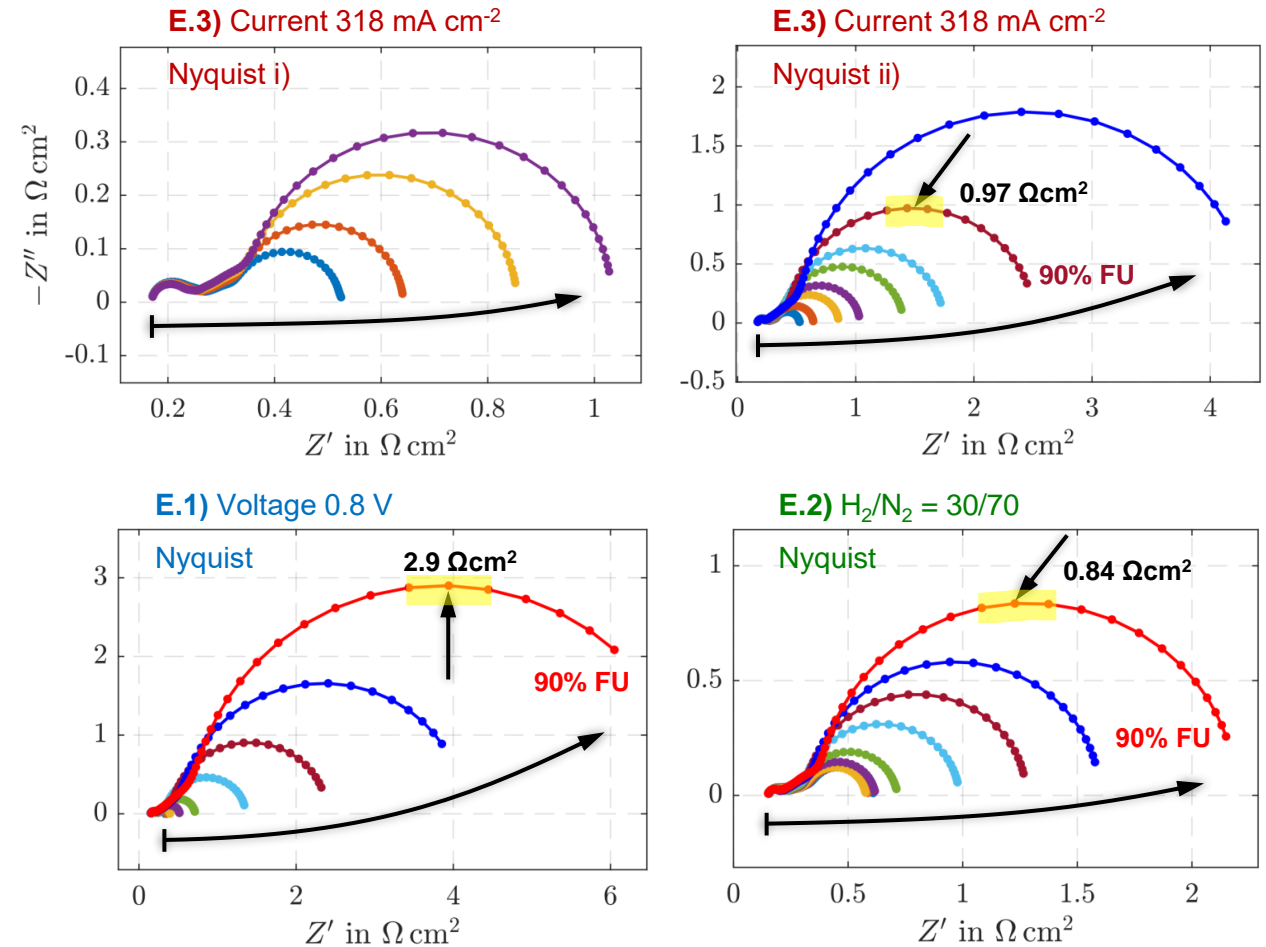


Fig.11: Nyquist plots of experiments on fuel starvation.

Fuel Starvation (SOFC)

Introduction
Exp. method
Modeling
Exp. results
Model results
Conclusion

	No	FU %
1		50
2		65
3		75
4		80
5		84
6		87
7		90
8		93
9		

- **Bode:** Low-frequency peak \uparrow and shifts to lower frequencies as FU \uparrow
- **DRT:** Gas conversion peak P2 \uparrow and shifts from 10^1 to 10^0 as FU \uparrow
- **THD:** THD \uparrow the \downarrow the frequency and \uparrow FU, for $f < 2$ Hz
THD above 1% threshold (healthy state) for FU $> 80\%$
max THD 9.3% at 87mHz for 93% FU

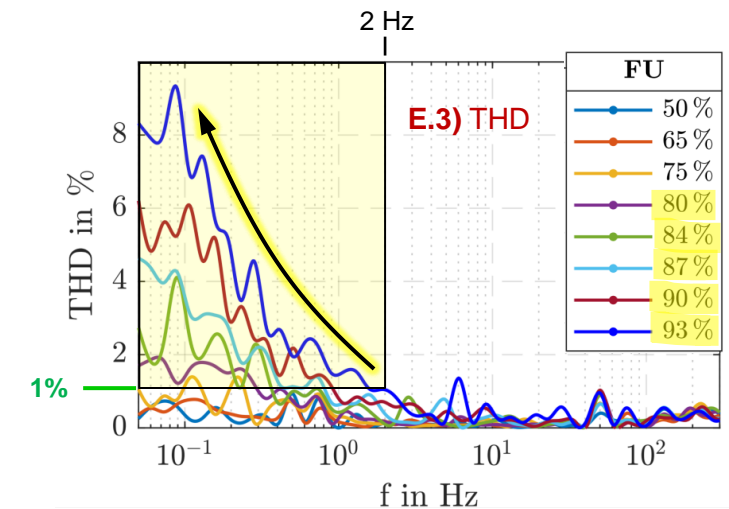
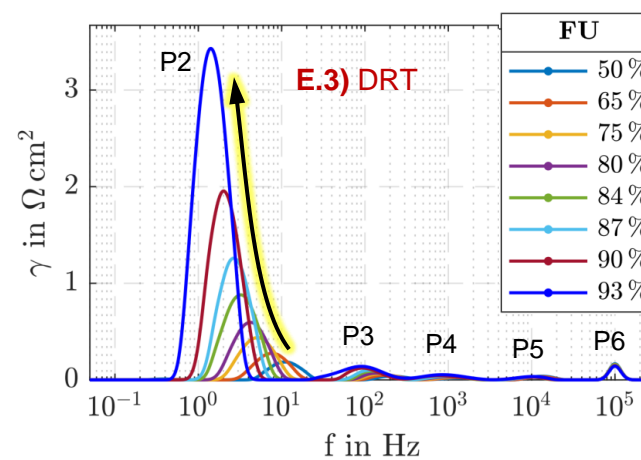
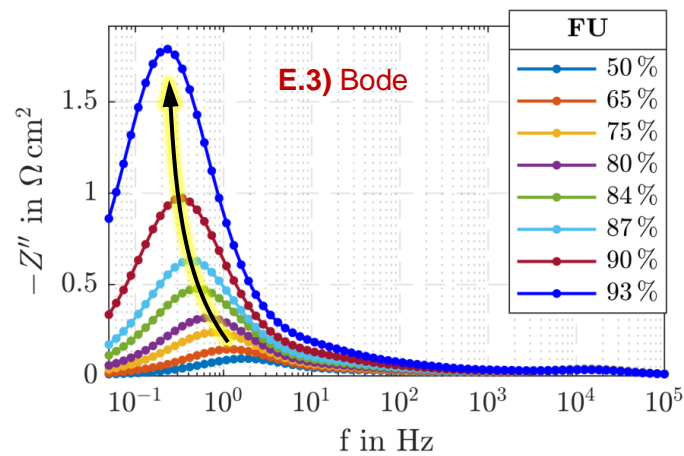


Fig.12: Bode, DRT, and THD plot of experiment 3 on fuel starvation.

Steam Starvation (SOE)

- Introduction
- Exp. method
- Modeling
- Exp. results**
- Model results
- Conclusion

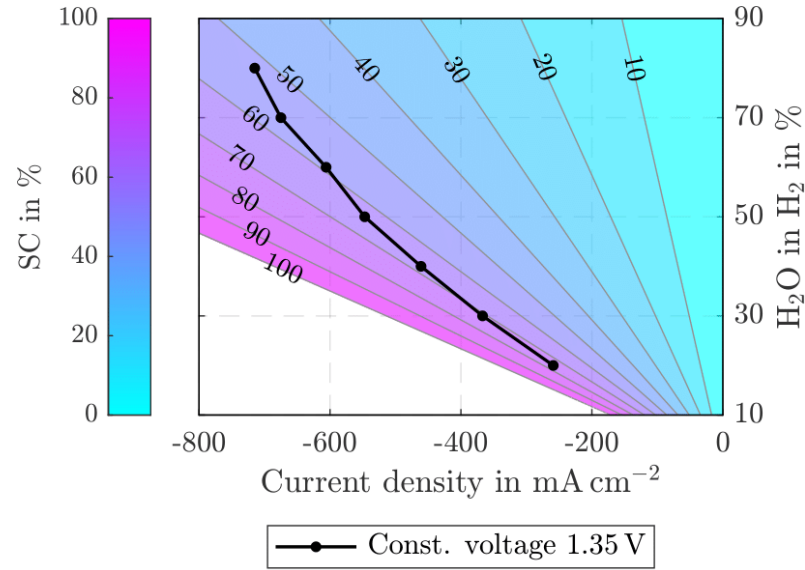


Fig.13: SC with current density and composition ($150 \text{ Nm l min}^{-1}$, 12.57 cm^2).

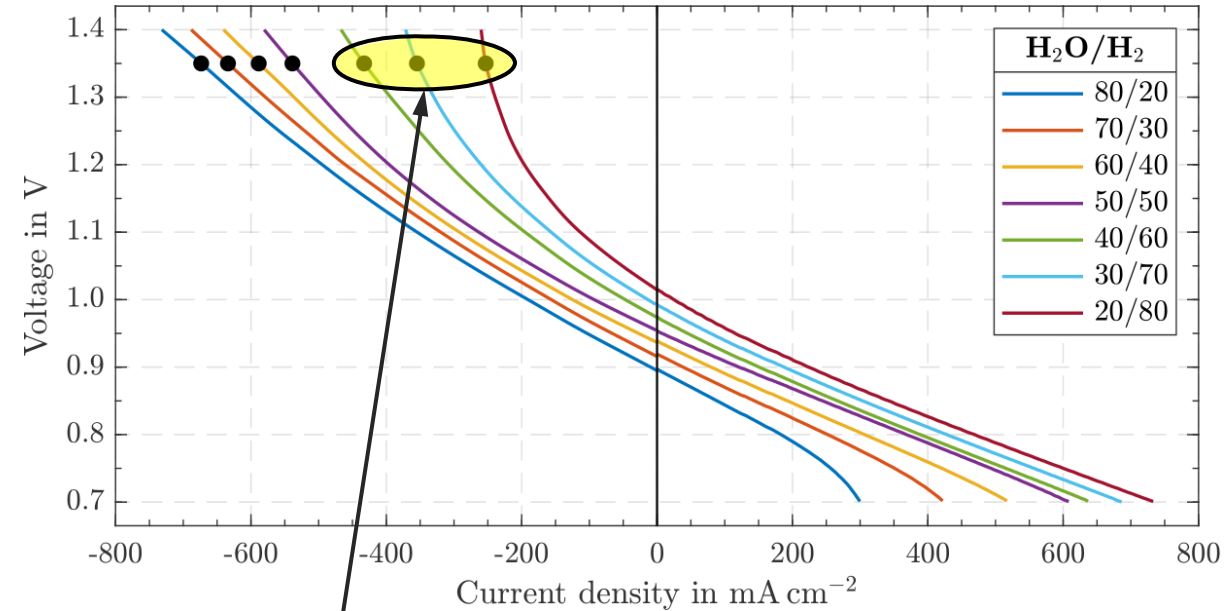


Fig.14: jV curves of steam starvation. Dots indicate operating points of EIS/THD measurements.

Steam Conversion:
$$SC = \frac{jA_{cell}}{z_e F \dot{n}_{\text{H}_2\text{O}}} \quad \text{Eq. (9)}$$

- For **SC > 67%** significant voltage rise ($\uparrow \eta_{\text{conc}}$)

Steam Starvation (SOE)

- Introduction
- Exp. method
- Modeling
- Exp. results
- Model results
- Conclusion

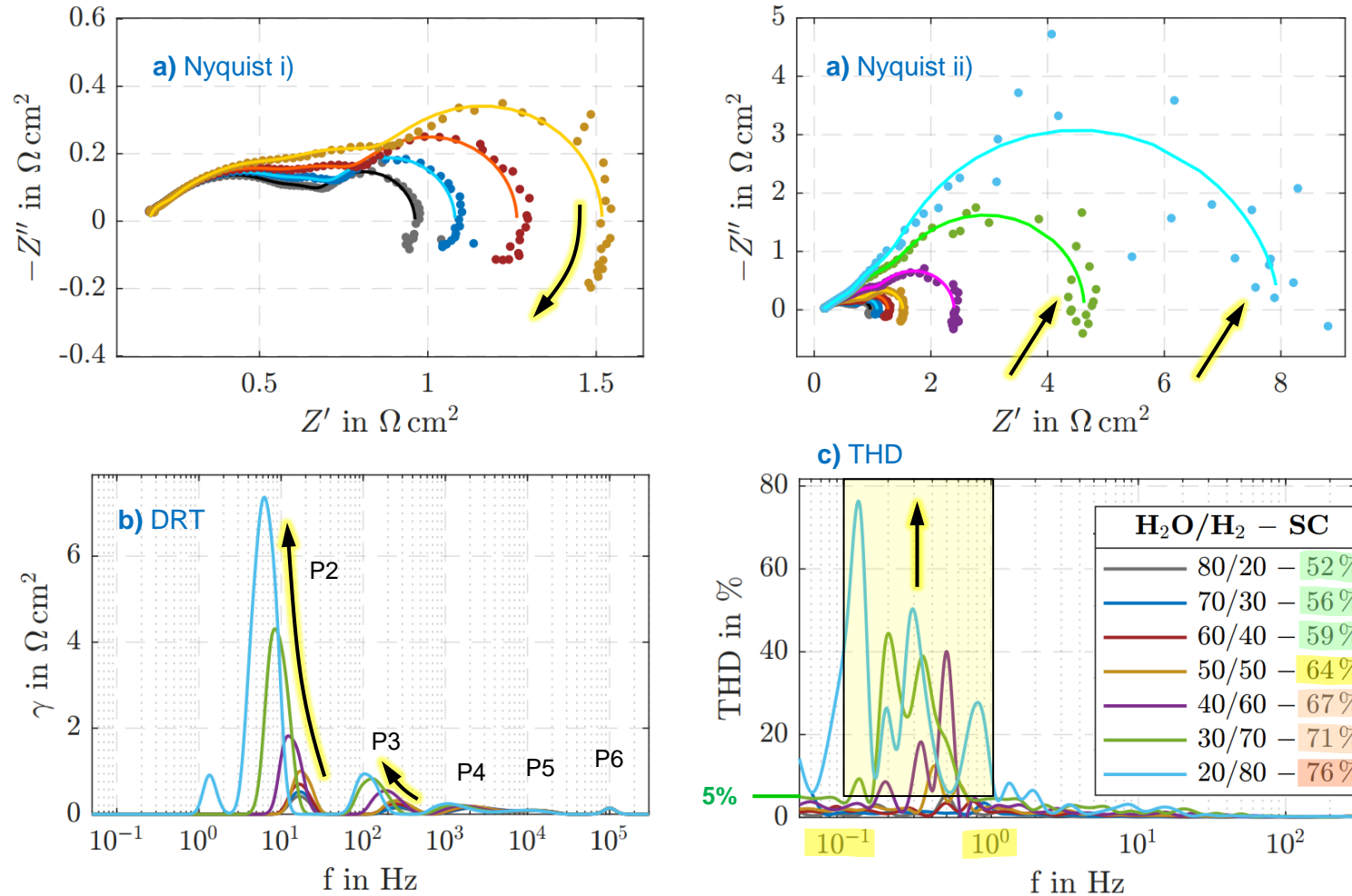
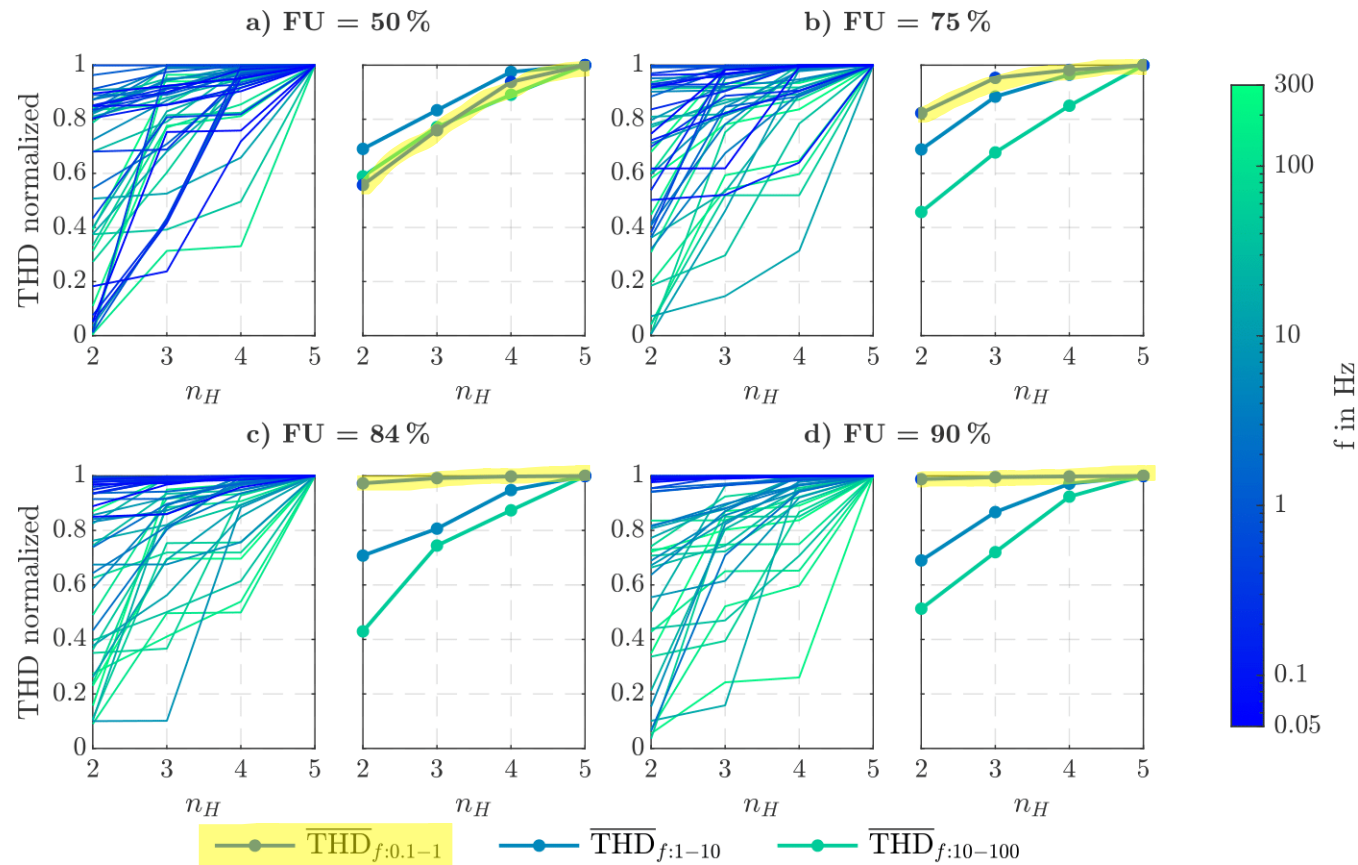


Fig.15: EIS, DRT, and THD results of steam starvation at 1.35V, Amp = 50mV.

- **Nyquist:**
“Pseudo-inductive” loop;
For SC $\geq 71\%$ (H₂ $\leq 30\%$)
immense fluctuations in
raw data
- **DRT:**
P2 and P3 \uparrow and shift to
lower freq. as SC \uparrow
- **THD:**
Threshold $\approx 5\%$,
THD $\uparrow\uparrow$ between 0.1–1Hz
as SC \uparrow ;
Max THD 76% at 125mHz
for 76% SC

THD – Number of Harmonics

- Introduction
- Exp. method
- Modeling
- Exp. results
- Model results
- Conclusion



The increase in THD at low frequencies (< 2 Hz) due to fuel starvation stems almost exclusively from the **2nd harmonic**. All others are negligible.

Fig.16: Evolution of THD index with harmonics used, normalized to highest THD($n_H = 5$). Operating points from E1.3 (const. current 318 mA cm^{-2} and Amp = 5%).

Model Validation

Introduction

Exp. method

Modeling

Exp. results

Model results

Conclusion

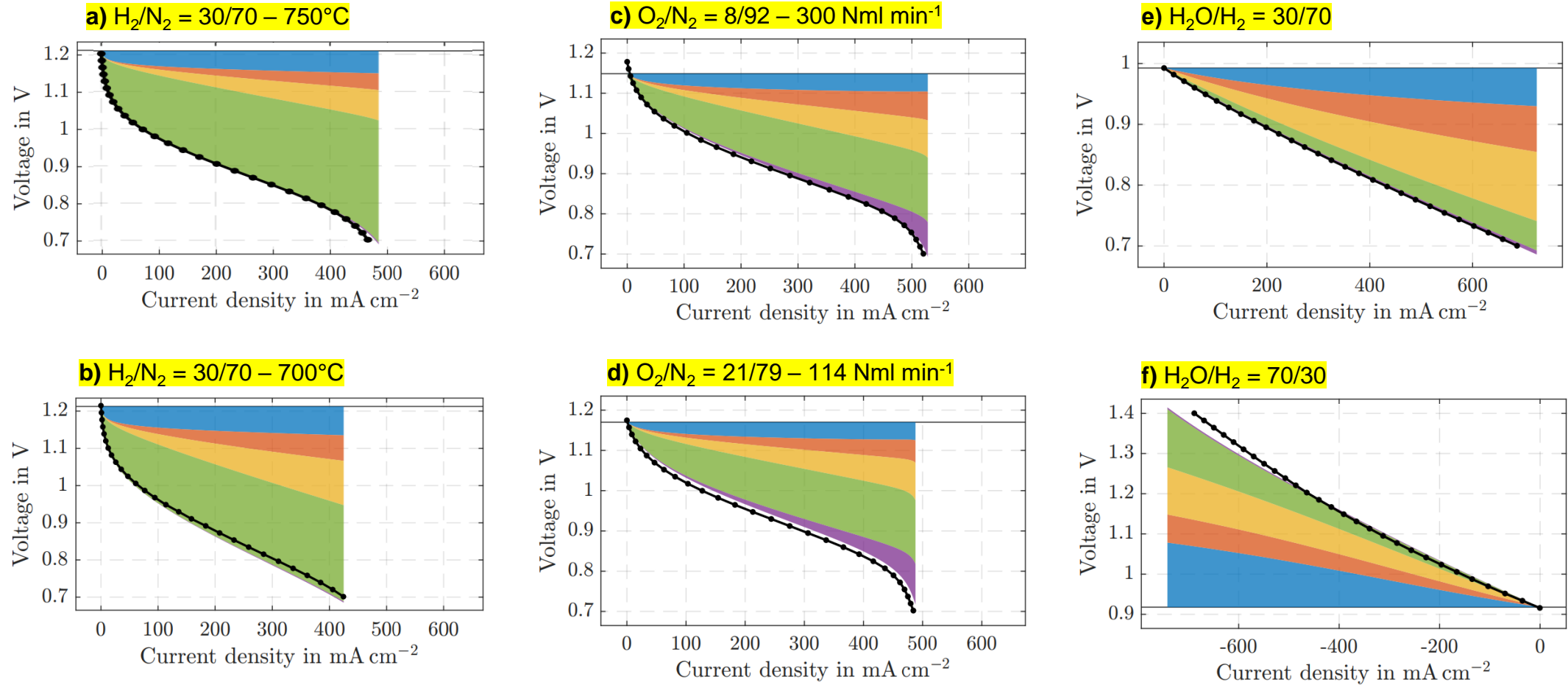


Fig.17: Simulation versus measurements a) fuel starvation, b) temperature, c) and d) air starvation, e) and f) humid fuel.

- Introduction
- Exp. method
- Modeling
- Exp. results
- Model results**
- Conclusion

Simulation

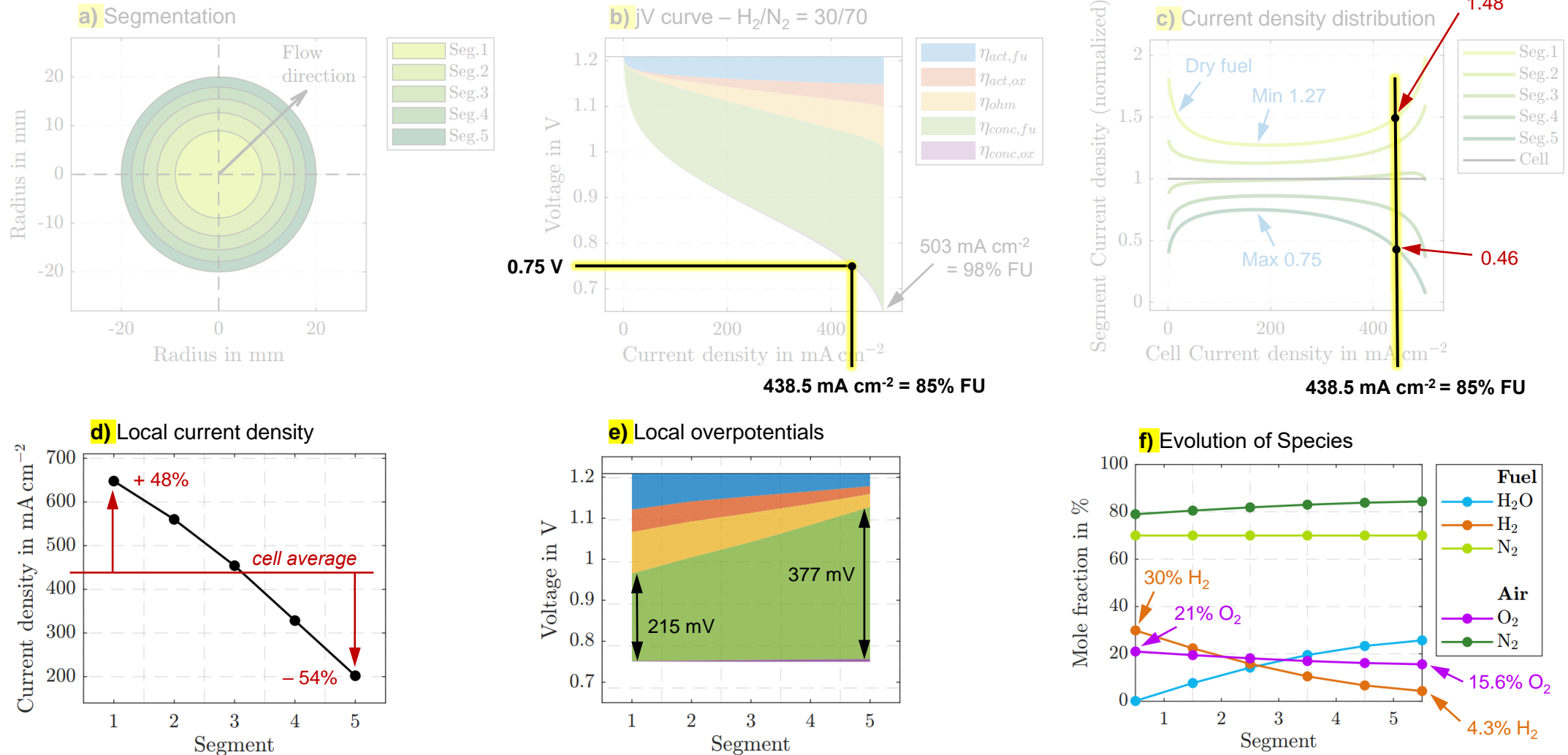


Fig.18: Simulation for H₂/N₂ = 30/70, 150 Nml min⁻¹ fuel flow rate, O₂/N₂ = 21/79, 300 Nml min⁻¹ air flow rate, 750°C cell temperature, outward fuel flow.

Conclusion

Introduction

Exp. method

Modeling

Exp. results

Model results

Conclusion

▪ Experimental

- Extensive characterization of reactants starvation in SOFC and SOE modes
- Tools: Polarization curve, EIS & DRT, and THD (each having advantages & drawbacks)

▪ Modeling

- 2D steady-state model → Large local disparities during critical conditions

➤ **EFCF Presentation**
by Gerald Hammerschmid
On Friday 10:15

▪ Impact

- **Understanding** of critical conditions and **how to detect** them (novelty THD)
- Improve State-of-Health monitoring → Prevent degradation → **Increase lifetime**
- Use model to propose **safe operating points** free of local extremes

▪ Outlook

- Accelerated Stress Tests
- Other failure modes
- Stacks & systems
- Transient model



This work has received funding from the Fuel Cells and Hydrogen 2 Joint Undertaking (now Clean Hydrogen Partnership) under grant agreement N° 101007175 (REACTT), 875047 (RUBY) and 825027 (AdAstra) and Hydro-Québec Research Institute (IREQ). This Joint Undertaking receives support from the European Union's Horizon 2020 research and innovation program, Hydrogen Europe and Hydrogen Europe research.

Comparison of Tools

BACKUP SLIDE

	jV	EIS & DRT	THD
Information	Global performance/SoH No identification of individual processes	In-depth characterization Deconvolution of processes by time charact. Identification of criticalities and causes	Severity of monitored criticalities Limited to certain criticalities
Time	Fast (< 3min)	Slow (> 15min) to obtain sufficient spectrum	Fast (1-2min) to monitor relevant frequencies
System Availability	Interrupted	In steady-state mode OK In dynamic mode not possible	In steady-state mode OK In dynamic mode not possible
Main Purpose	Characterization	Characterization	Monitoring
Application	Commercial	Laboratory	Emerging Commercial
Reliability / Reprod.	Very Good	Good	Fairly Good
Equip. Requirements	Low	High	High(er)
Usability	Simple	Sophisticated	Sophisticated

Working Principle

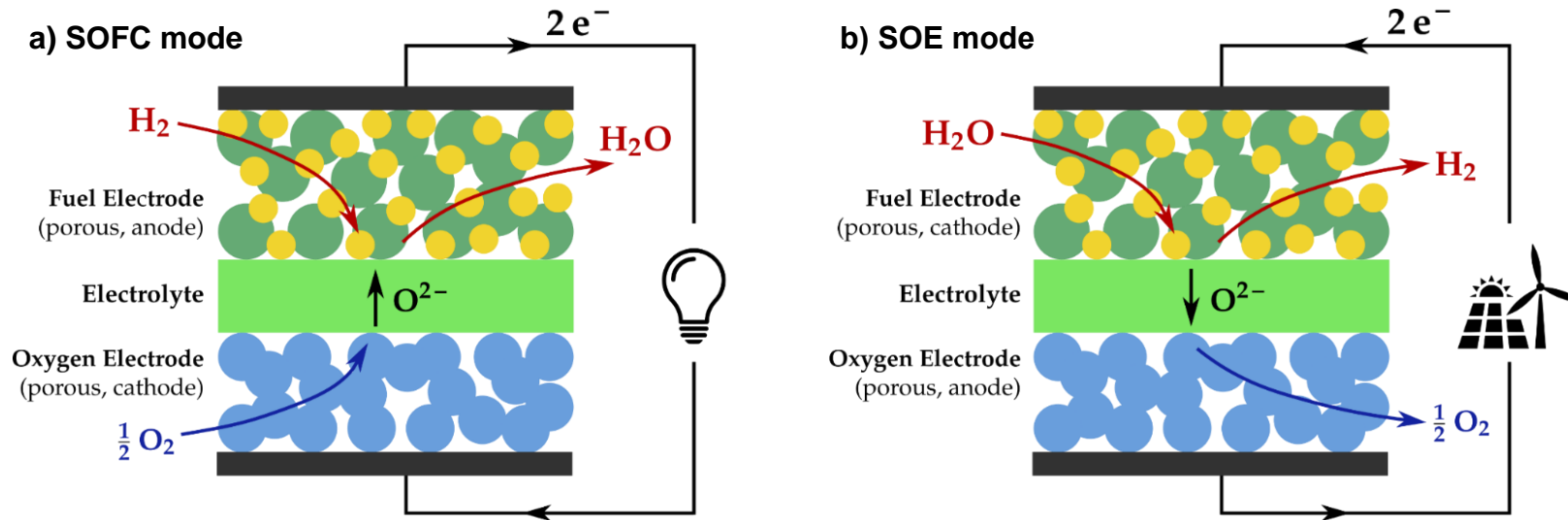


Fig.3: Schematic representation of the working principle of a SOFC in a) SOFC mode and b) SOE mode.

- Temperature: 600 – 1000°C
- Reactions: at triple-phase-boundary (TPB)
- Fuel flexibility: H_2 , NH_3 , CO , CH_4 ...
- Reversibility: fuel cell \leftrightarrow electrolyzer mode
- Dense, ceramic electrolyte: YSZ
- Porous electrodes
 - Fuel side: Ni-YSZ
 - Air side: LSM, LSM-YSZ, LSCF, LSCF-GDC

BACKUP
SLIDE

Causes for Failure and Degradation

BACKUP SLIDE

- Causes for failure:

current
voltage

temperature

gas composition

leakage

load-cycles

unpredicted shut-down

defects in balance-of-plant (BoP) ...

- Degradation:** Deterioration of cell performance over time

Fuel Electrode:

- *Ni-oxidation*
- *Ni-agglomeration*
- *Carbon deposition*
- *Poisoning: S, Cl, Si, Na, Al*

Oxygen Electrode:

- *Delamination of electrode/electrolyte interface*
- *Secondary phases: SrZrO₃, Cr₂O₃*
- *Cr evaporation*

Electrolyte:

- *Decomposition of YSZ*
- *Reduction of YSZ*

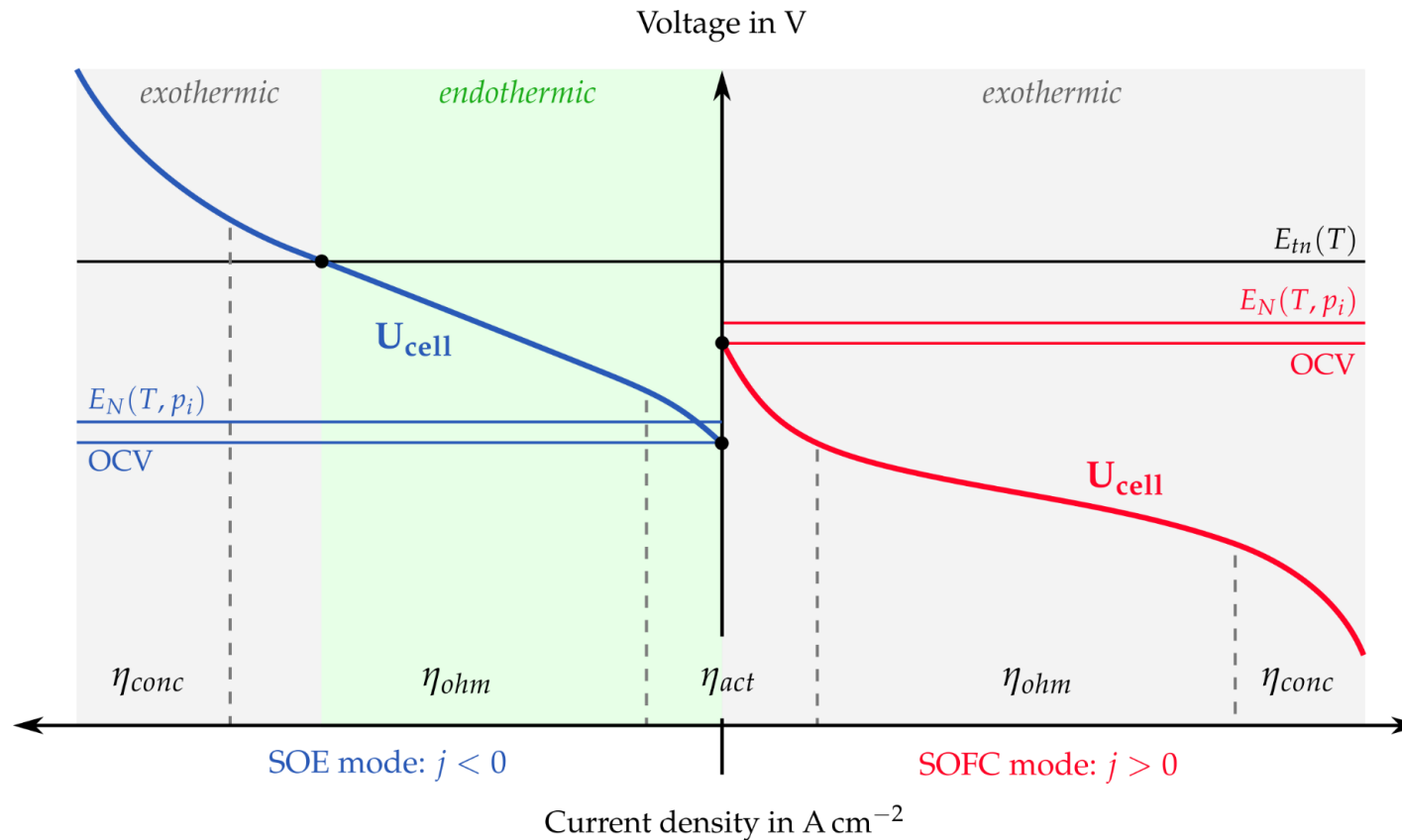
Experimental investigation of fuel-, air-, steam starvation:

- Polarization curves (jV)
- Electrochemical Impedance Spectroscopy (EIS) and Distribution of Relaxation Times (DRT)
- Total Harmonic Distortion (THD)

2D, steady-state **simulation model** with MATLAB

SCOPE

Polarization Curve (jV)



$$E_{tn} = -\frac{\Delta_r H(T)}{z_e F} \quad \text{Eq. (1)}$$

$$E_N = -\frac{\Delta_r G(T, p^0)}{z_e F} - \frac{RT}{z_e F} \ln \left(\prod_i \left(\frac{p_i}{p^0} \right)^{v_{st,i}} \right) \quad \text{Eq. (2)}$$

$$U_{cell} = OCV - \eta_{act} - \eta_{ohm} - \eta_{conc} \quad \text{Eq. (3)}$$

$$ASR_{local}(j^*) = \left. \frac{dU}{dj} \right|_{j=j^*} \quad \text{Eq. (4)}$$

Fig.2: Typical current-voltage (jV) characteristic known as polarization curve.
(Note: Same temperature but different gas composition in each mode, therefore different Nernst voltage.)

(STP: 25°C, 1.01325 bar)

Electrochemical Impedance Spectroscopy (EIS)

BACKUP SLIDE

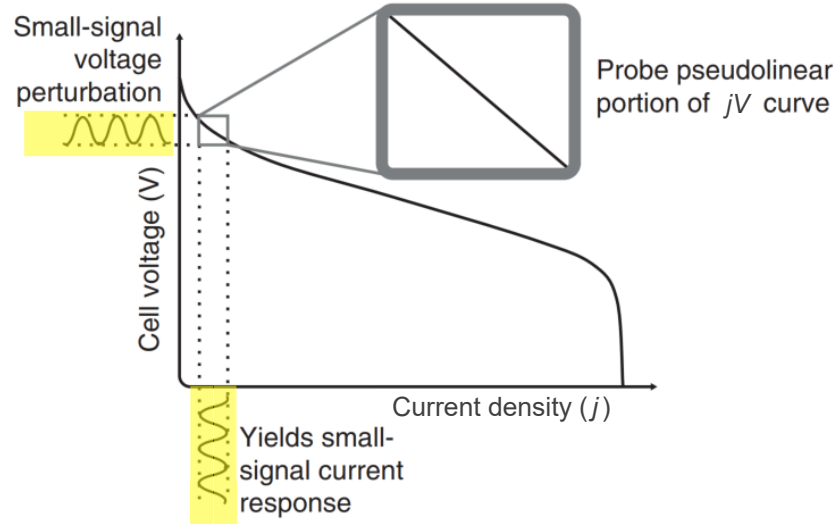


Fig. 5: EIS method from "Fuel Cell Fundamentals" (O'Hayre et al., 2016).

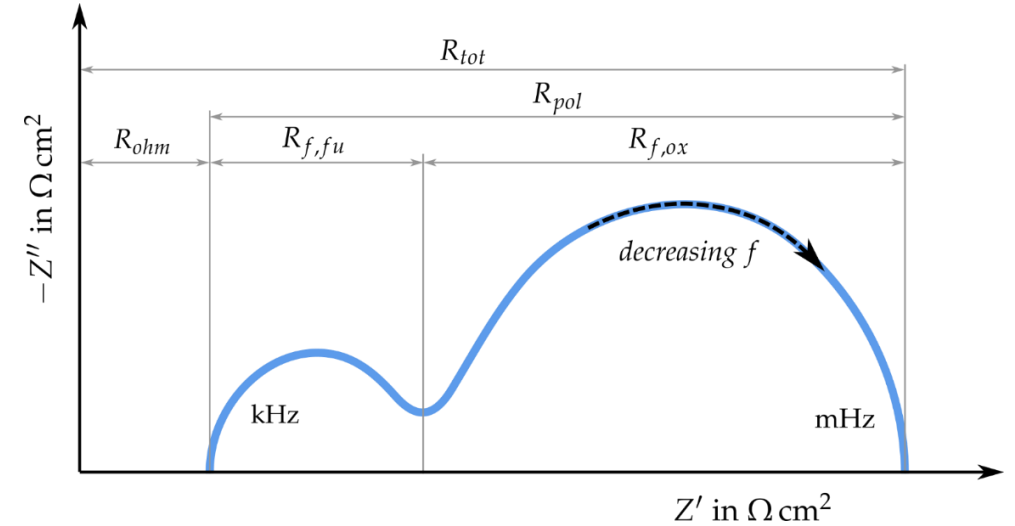


Fig. 6: Schematical representation of an impedance spectrum as Nyquist plot.

Impedance:
$$Z(\omega) = \frac{U(t)}{j(t)} = \frac{\hat{U} \sin(\omega t + \phi)}{\hat{j} \sin(\omega t)} = \frac{\hat{U} e^{i(\omega t + \phi)}}{\hat{j} e^{i\omega t}} = \hat{Z} e^{i\phi} = \hat{Z} (\cos \phi + i \sin \phi) \quad \text{Eq. (1)}$$

DRT (Distribution of Relaxation Times):

$$Z_{\text{DRT}}(\omega) = R_{ohm} + \int_{-\infty}^{\infty} \frac{\gamma(\ln \tau)}{1 + i\omega\tau} d(\ln \tau) \quad \text{Eq. (2)}$$

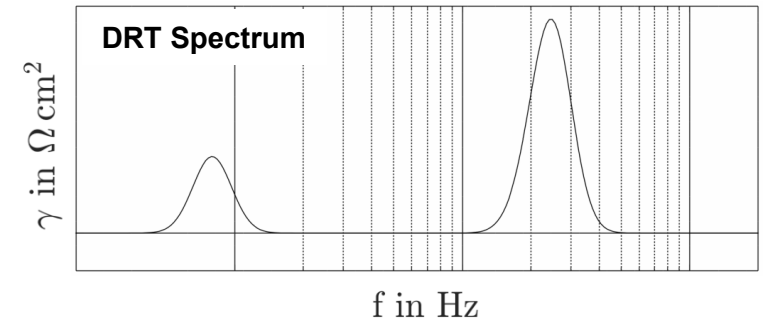
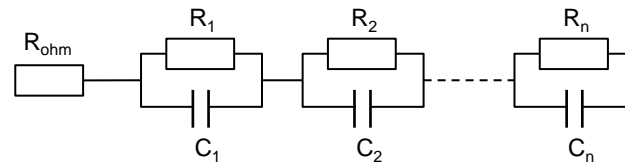


Fig. 7: Schematical representation of a DRT spectrum.

Test Rig

BACKUP SLIDE

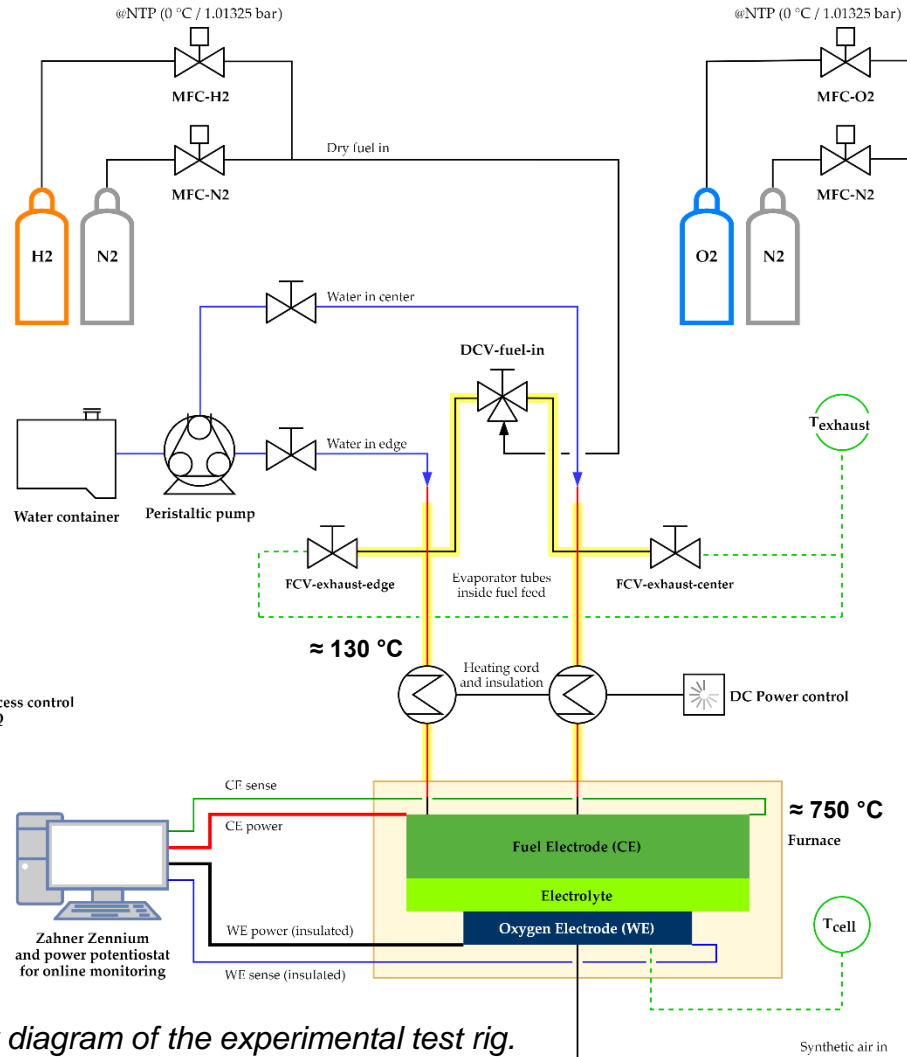


Fig.8: Process flow diagram of the experimental test rig.

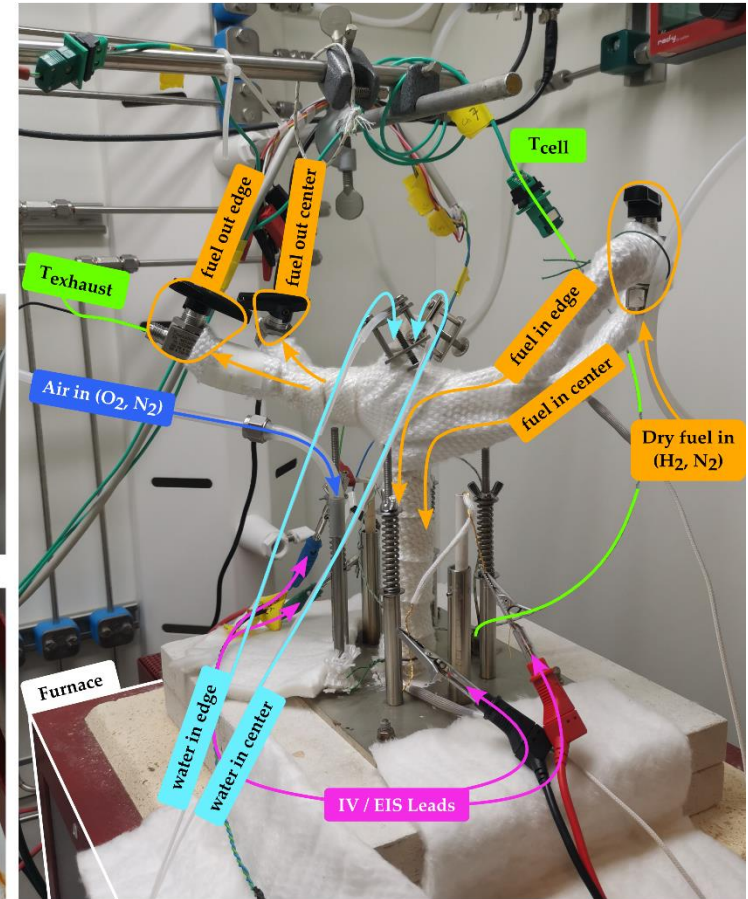
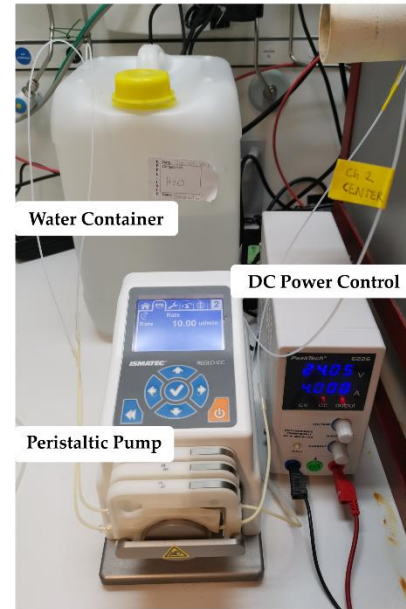


Fig.9: Photos of the experimental test rig.

Test Rig Modifications

BACKUP SLIDE

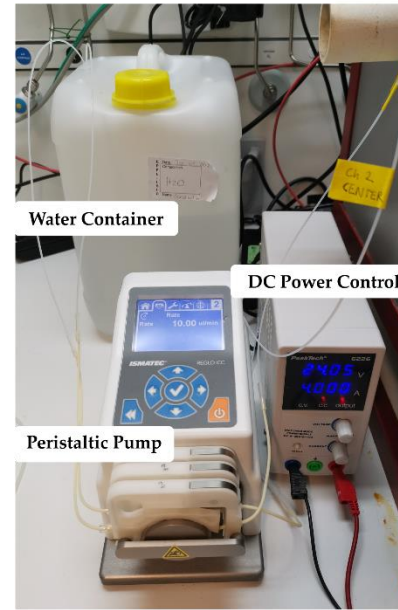
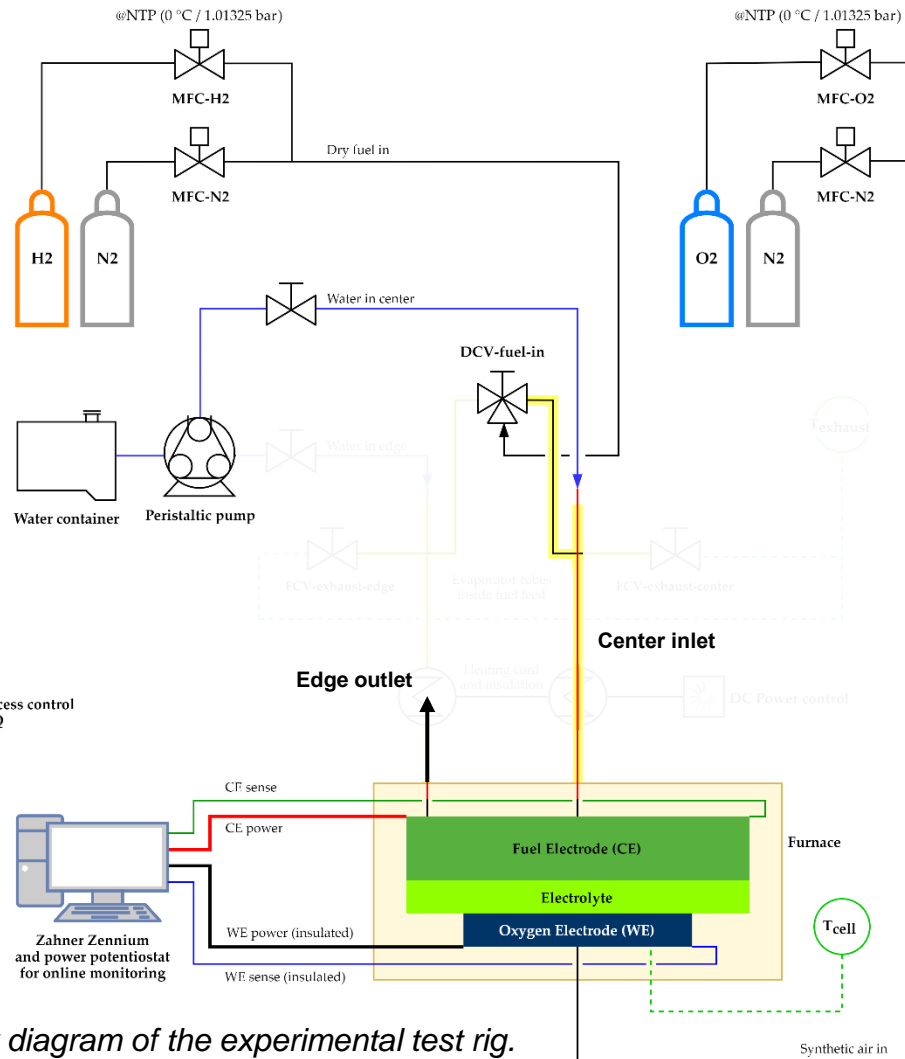


Fig.8: Process flow diagram of the experimental test rig.

Fig.9: Photos of the experimental test rig.

Design of Experiments

BACKUP
SLIDE

Tab.1: List of experiments.

No	Name
1	Fuel Starvation
1.1	Constant Voltage
1.2	Constant Composition
1.3	Constant Current
2	THD Sensitivity
2.1	Signal Amplitude
2.2	Number of Harmonics
3	Temperature
4	Flow Direction
5	Air Starvation
5.1	Varying Air Composition
5.2	Varying Air Flow Rate
6	Steam Starvation

I. Failure mode →

THD Settings →

Operating conditions →

II. Failure mode →

III. Failure mode →

Tab.2: Default experiment parameter values.

Default:

- 750°C
- outward fuel flow
- 150 Nml min⁻¹ fuel flow rate
- 300 Nml min⁻¹ air flow rate
- H₂/N₂/H₂O fuel composition
- O₂/N₂ = 21/79 air composition
- 4 mV s⁻¹ jV sweep rate
- EIS galvanostatic in SOFC mode
- EIS potentiostatic in SOE mode
- 50mHz lower frequency limit
- 100kHz upper frequency limit
- 12 steps per decade
- 12 measure periods
- THD of first five harmonics

Modeling

BACKUP SLIDE

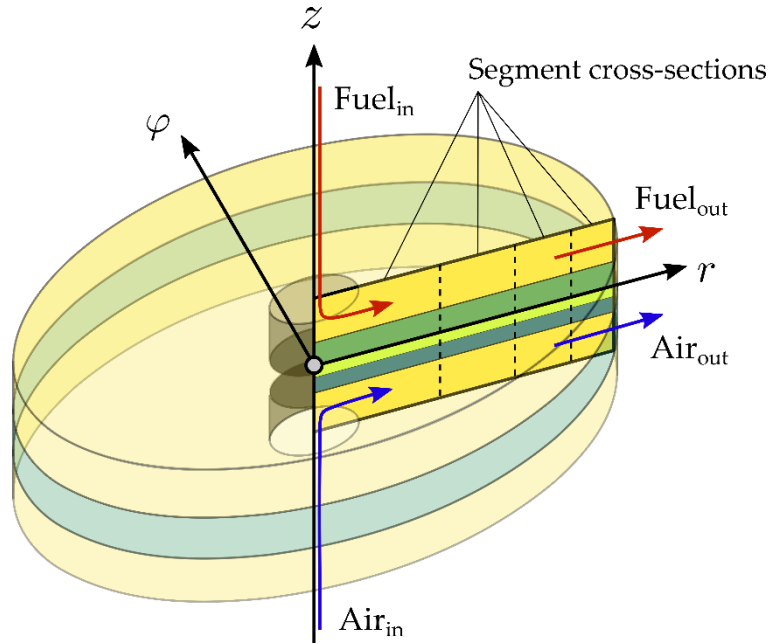


Fig.10: Computational domain based on the experimental setup.

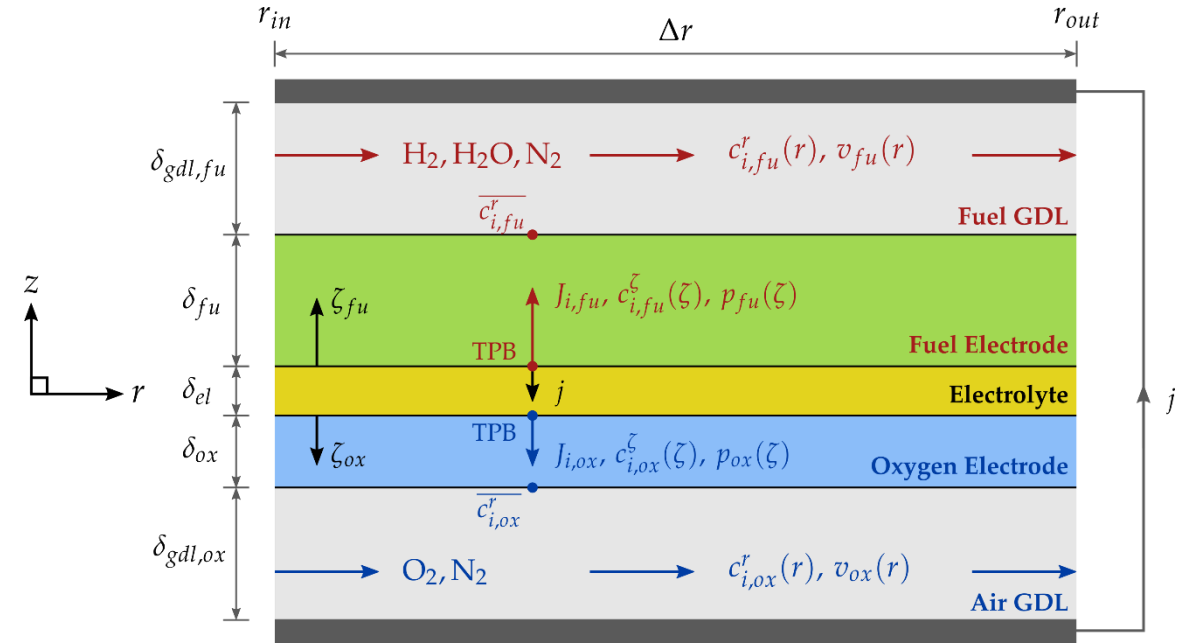


Fig.11: Schematic illustration of a segment cross-section.

▪ **Segmentation:**

- Coaxial cylinders
- Radial discretization such that all have same active area

▪ **Species balance in the GDL:**

$$\frac{1}{r} \frac{\partial}{\partial r} (rc_i^r v) = \frac{J_i}{\delta_{gdl}} \quad \text{Eq. (16)}$$

▪ **Species balance in the Electrodes:**

Dusty Gas Model (DGM)

$$\sum_{j \neq i} \frac{c_j^\zeta J_i - c_i^\zeta J_j}{c^\zeta D_{ij}^e} + \frac{J_i}{D_{iK}^e} = -\frac{\partial c_i^\zeta}{\partial \zeta} - \frac{B_g c_i^\zeta}{\mu D_{iK}^e} \frac{\partial p}{\partial \zeta} \quad \text{Eq. (17)}$$

Solution Algorithm

BACKUP SLIDE

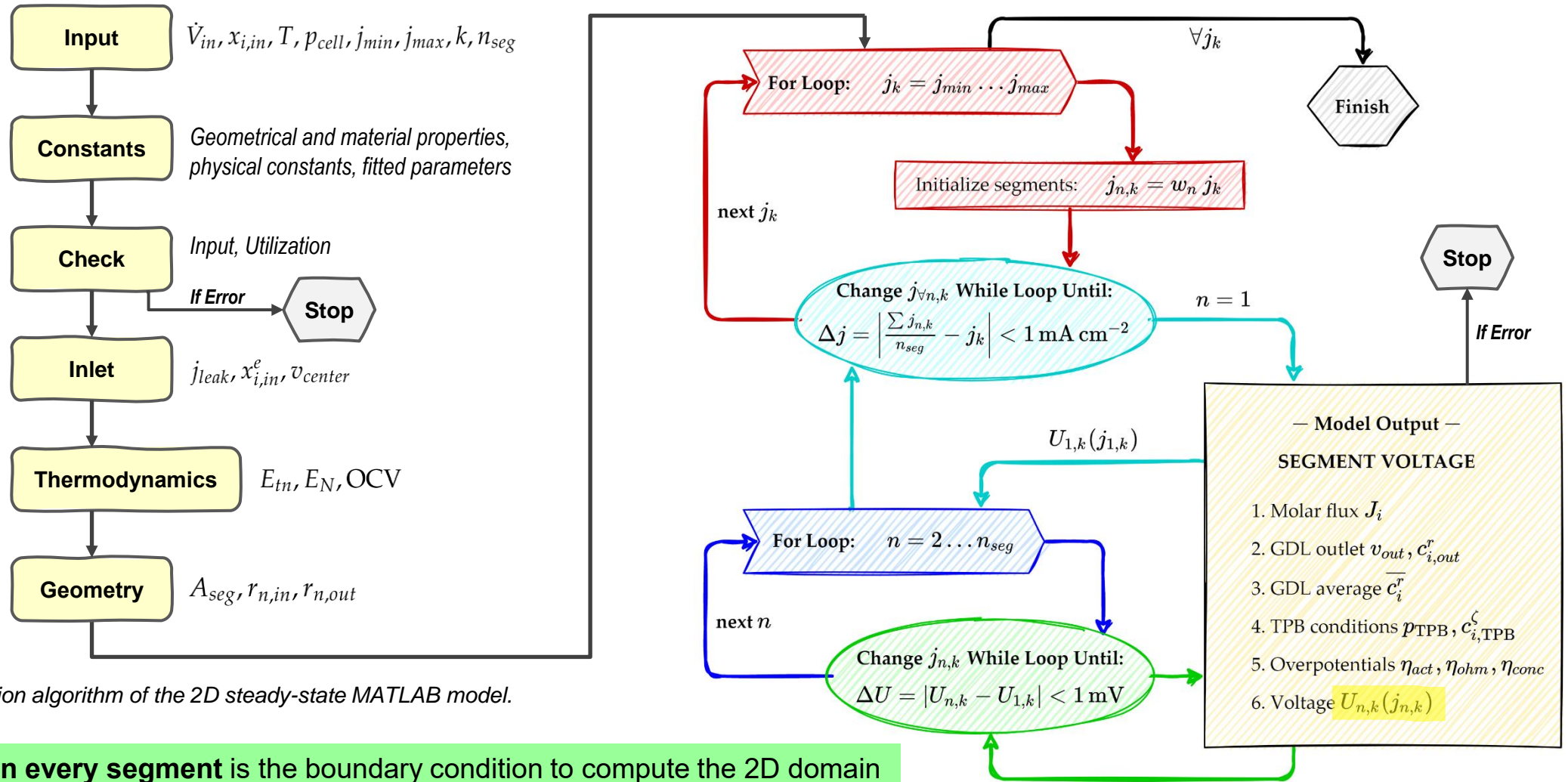
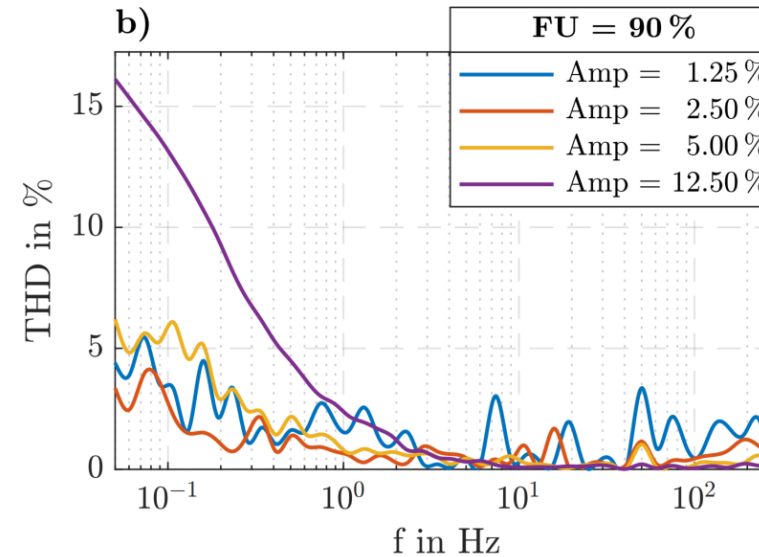
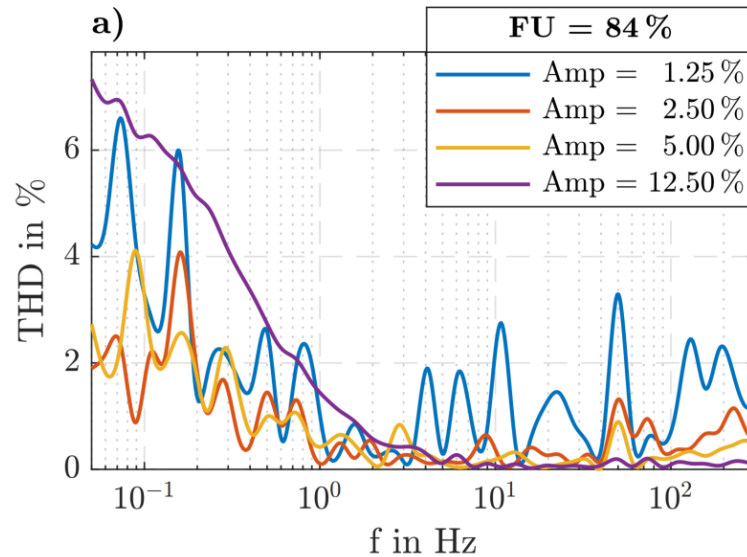


Fig.12: Flow chart of solution algorithm of the 2D steady-state MATLAB model.

The same voltage in every segment is the boundary condition to compute the 2D domain

THD – Excitation Signal Amplitude

BACKUP
SLIDE



$$j_{DC} = 4 \text{ A} \\ = 318 \text{ mA cm}^{-2}$$

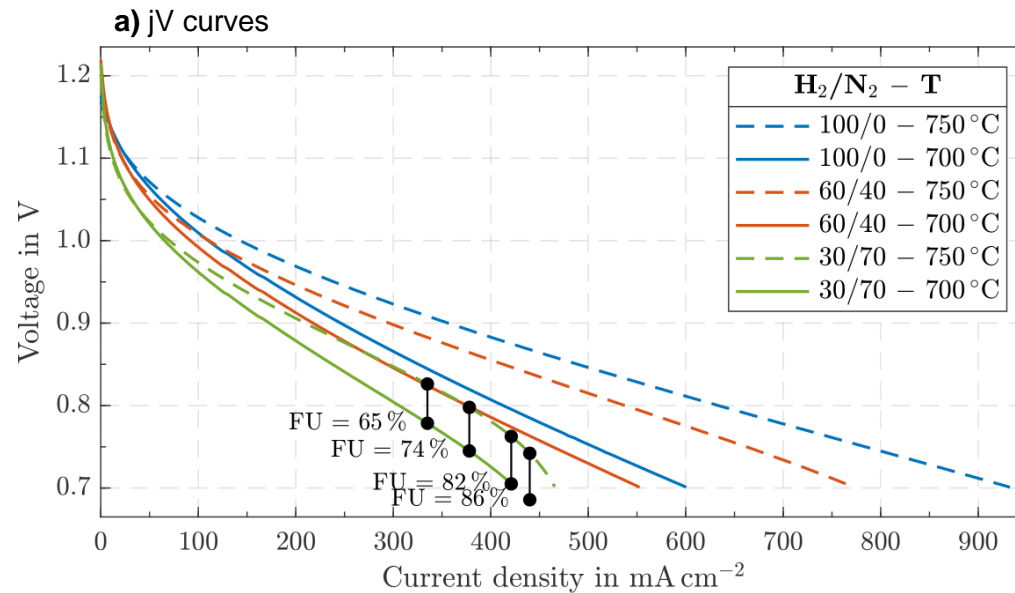
$$j_{AC} = 50, 100, \\ 200, 500 \text{ mA}$$

Fig.15: THD plot for different excitation signal amplitudes. Two operating points from E1.3 (const. current at 318 mA cm⁻²).

- **If amplitude small** → signal to noise ratio low and THD output corrupted by noise
- **If amplitude high** → non-linear operation *per se*, high distortion not necessarily from critical condition but due to measurement setting
- **Recommendation** → **approximately 5%**

Temperature

BACKUP
SLIDE



- $\eta_{ohm} \uparrow$ and $R_{ohm} \uparrow$ if $T \downarrow$
- high-frequency semicircle \uparrow if $T \downarrow$
- low-frequency semicircle $\neq f(T)$
- Charge transfer peaks P5 and P6 \uparrow if $T \downarrow$
- Gas conversion peak P2 $\neq f(T)$
- THD pattern similar

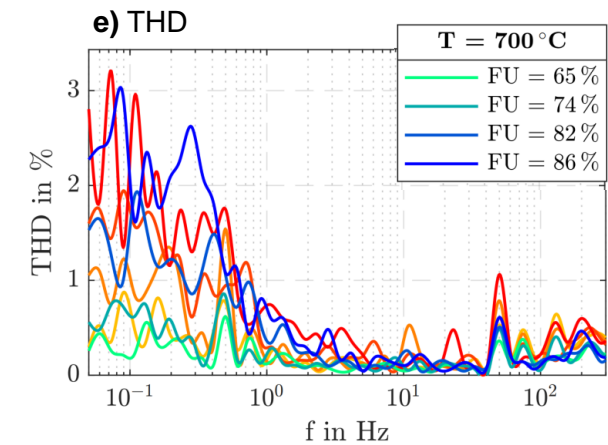
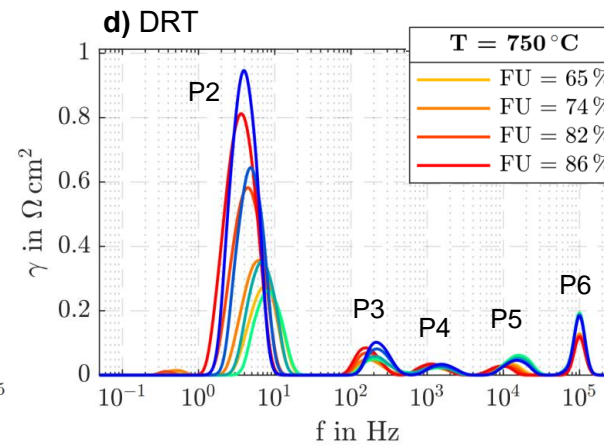
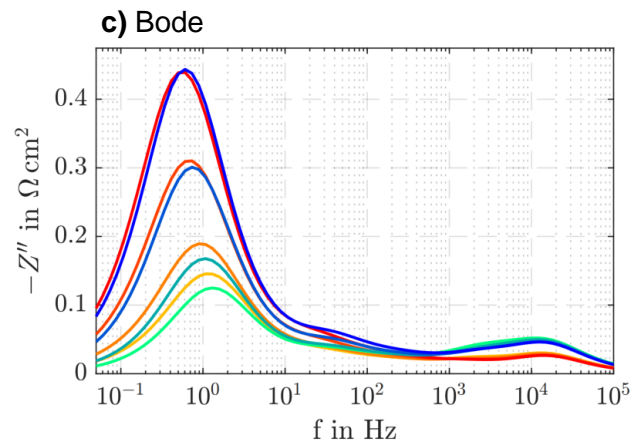
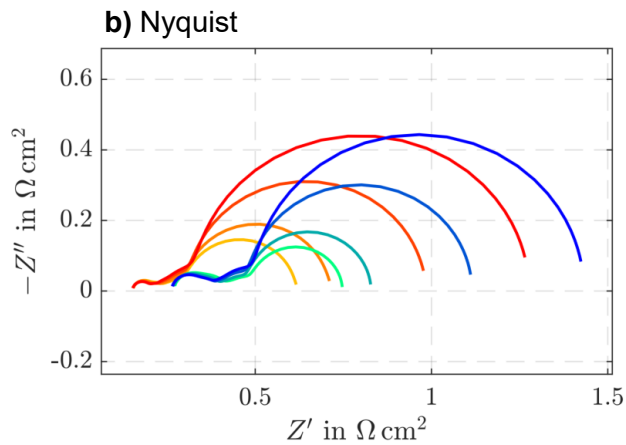


Fig.17: Comparison of 750 and 700°C cell temperature. jV curves of three compositions from E1.3 and EIS/THD measurements for four operating points from E1.2.

Flow Direction

BACKUP SLIDE

- OCV ↓ and T ↑ in inward flow
- η_{conc} ↑↑ in inward flow
- EIS, DRT, THD results of 48% inward ≈ 90% outward

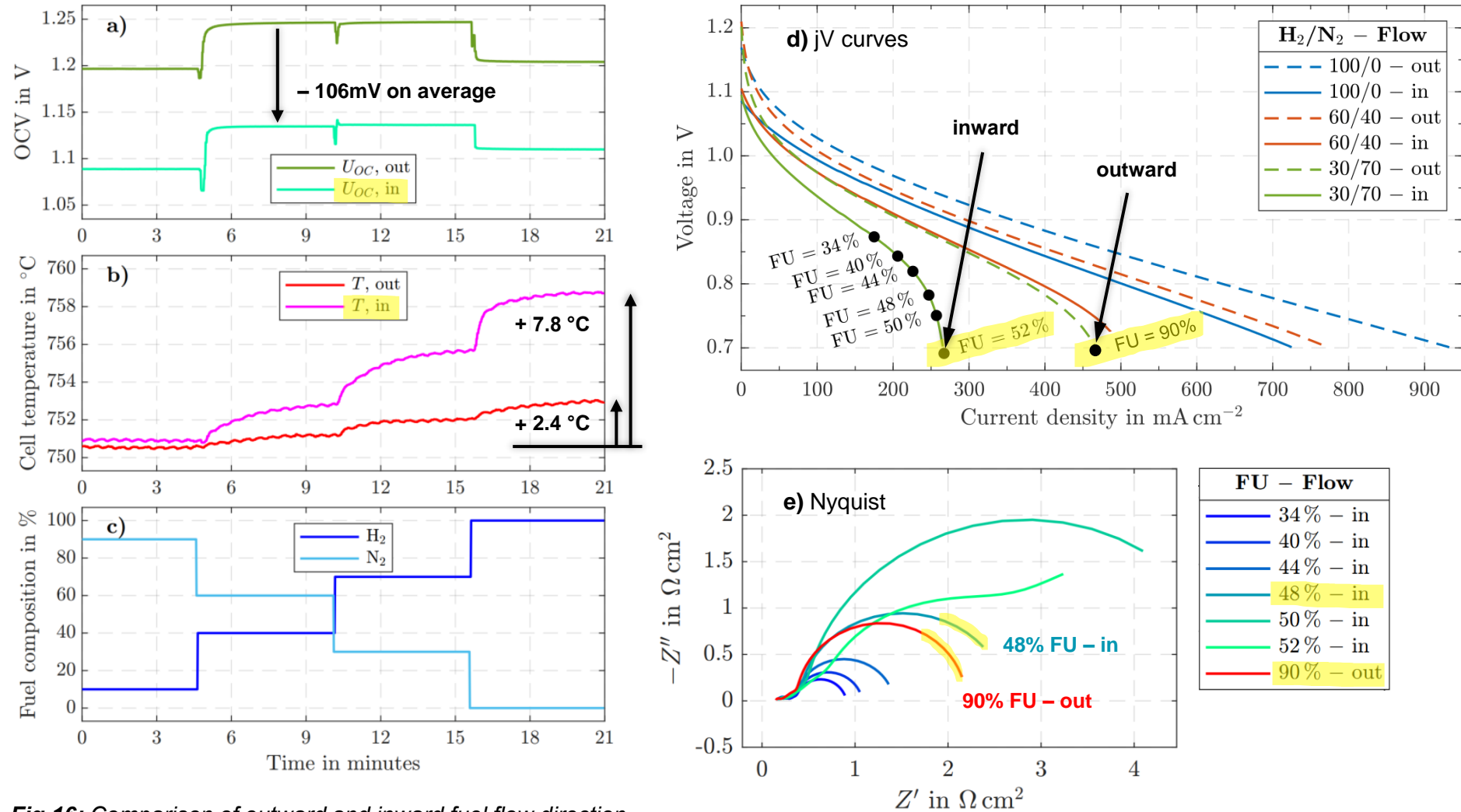


Fig.16: Comparison of outward and inward fuel flow direction.

BACKUP SLIDE

Air Starvation

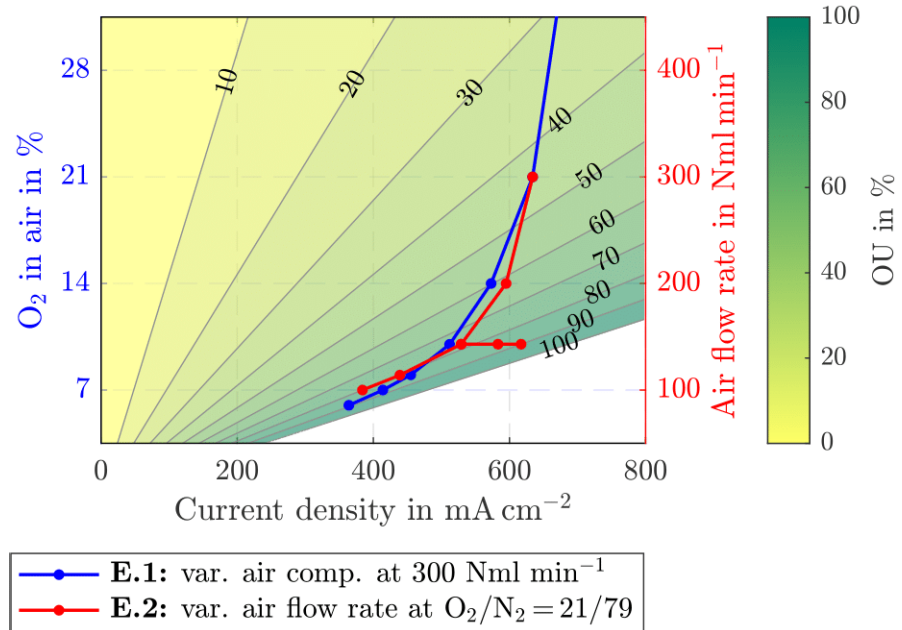


Fig.11: OU with current density, composition and air flow rate (12.57 cm², 150 Nml min⁻¹ fuel flow rate, 100% H₂).

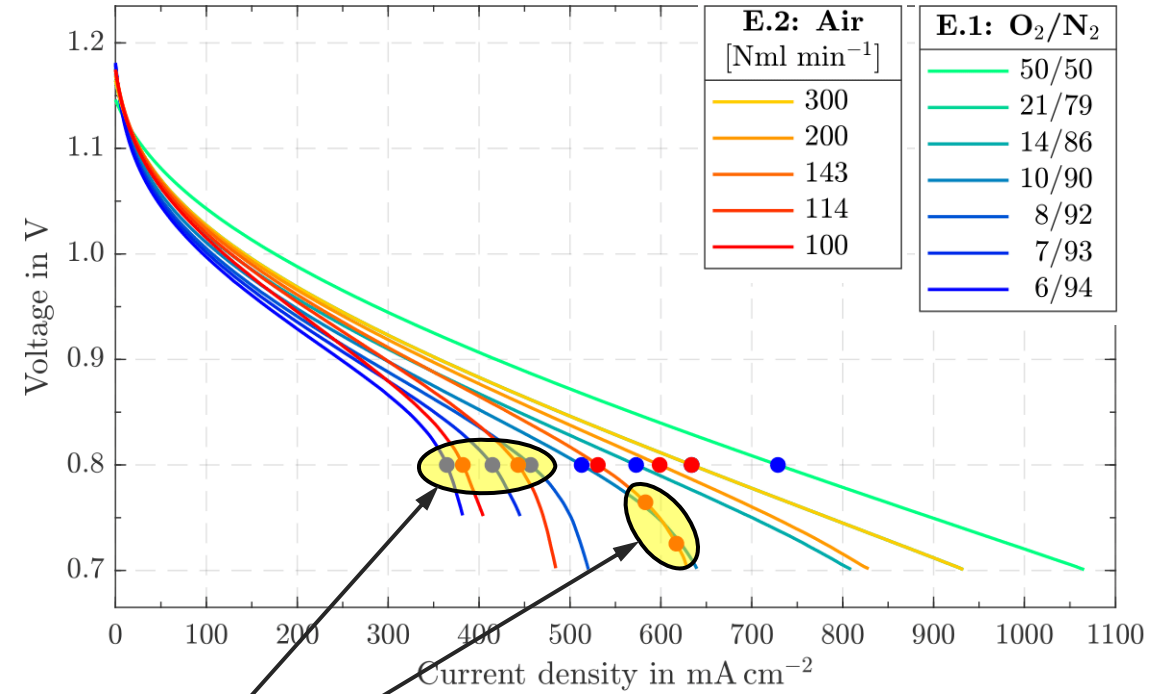


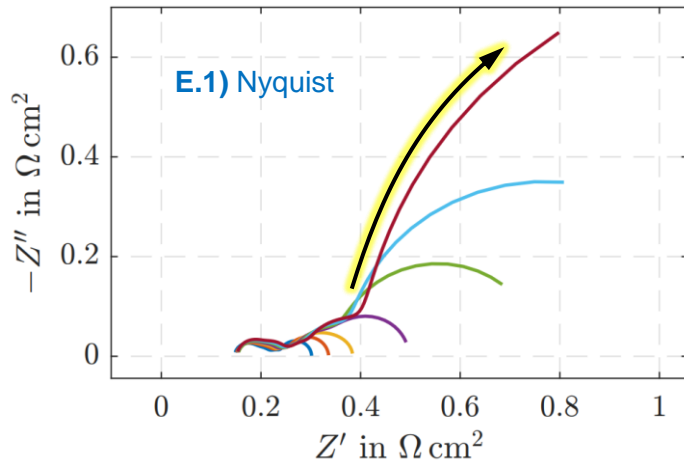
Fig.12: jV curves of air starvation. The dots indicate operating points of EIS and THD measurements.

Oxygen Utilization:
$$OU = \frac{jA_{cell}}{2z_e F \dot{n}_{O_2}} \quad \text{Eq. (12)}$$

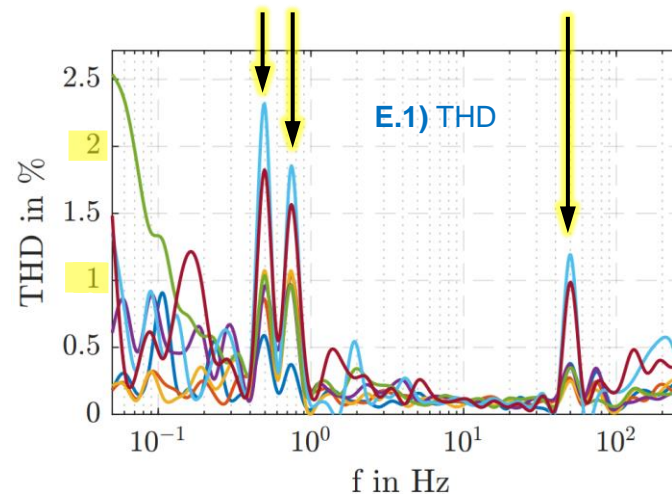
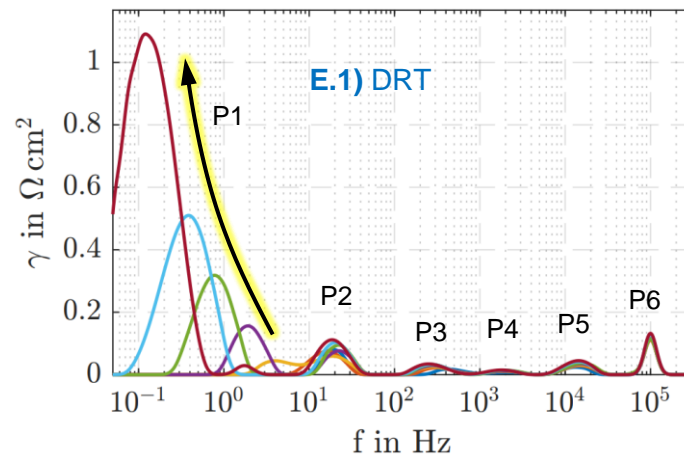
- For **OU > 80%** significant voltage drop (↑ η_{conc})

Air Starvation

BACKUP SLIDE



- **Nyquist:** 3rd semicircle at low frequencies for OU > 75%; Same behavior found in planar cells (Subotić et al, 2020, On the origin of degradation in fuel cells and its fast identification by applying unconventional online-monitoring tools)
- **DRT:** New peak P1 for OU > 75% (oxygen electrode diffusion)
- **THD:** Peaks at 500mHz, 750mHz, and 50Hz, but < 2.3% low → also visible in fuel starvation but overshadowed → setup-specific noise (e.g. furnace heating)

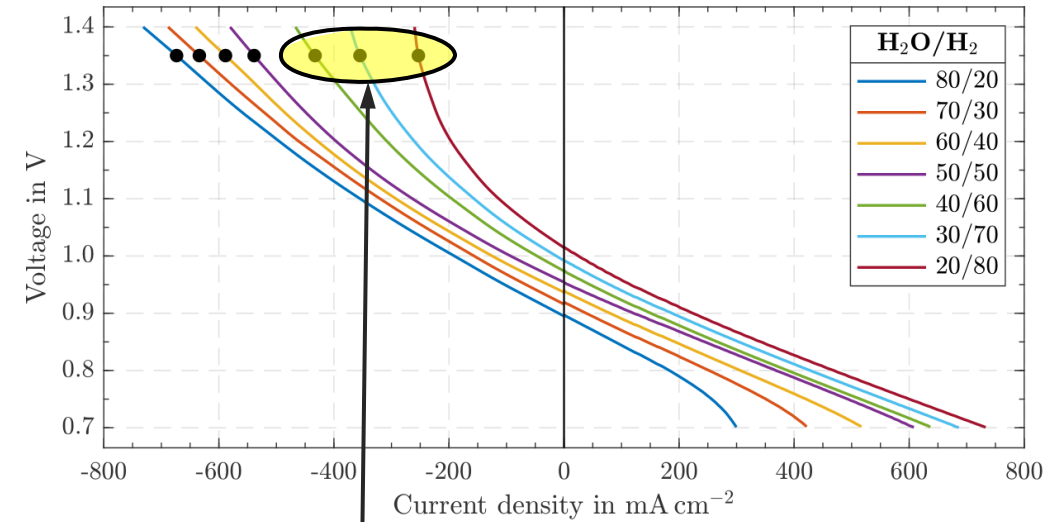
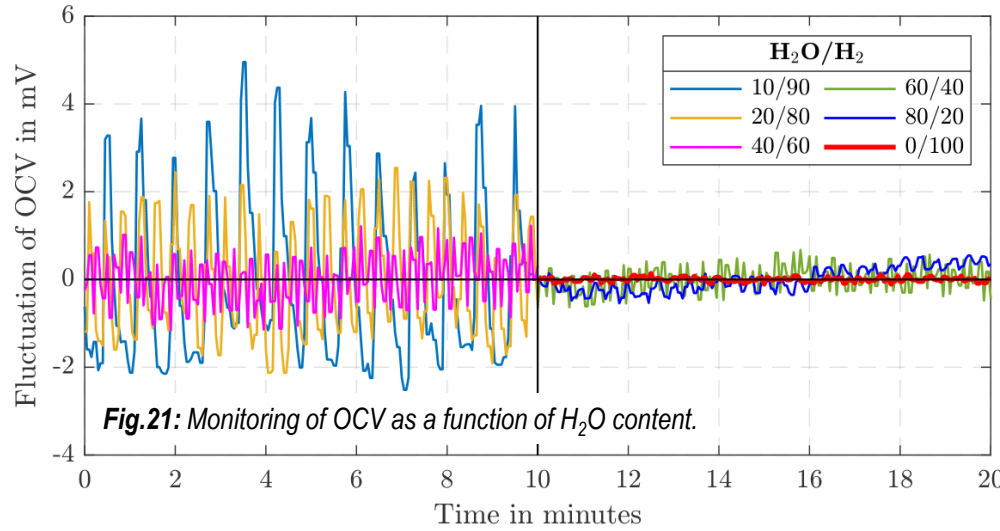


O ₂ /N ₂ – OU	
50/50	– 21 %
21/79	– 44 %
14/86	– 60 %
10/90	– 75 %
8/92	– 83 %
7/93	– 86 %
6/94	– 89 %

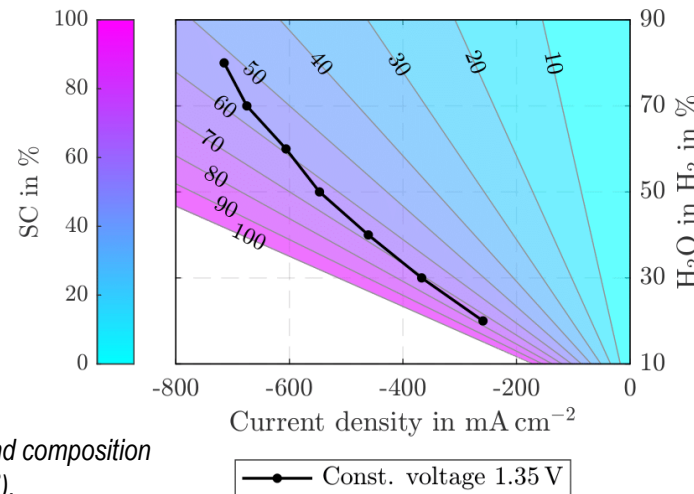
Fig.13: EIS, DRT, and THD results of air starvation E.1 with varying composition (O₂/N₂) at constant air flow rate of 300 Nml min⁻¹.

Steam Starvation

BACKUP SLIDE



- OCV more stable if H₂O flow rate higher



- For **SC > 67%** significant voltage rise (↑ η_{conc})

Steam Conversion:
$$SC = \frac{j_{A_{cell}}}{z_e F \dot{n}_{H_2O}} \quad \text{Eq. (18)}$$

Model Parameter Fitting

BACKUP SLIDE

- Ohmic resistance R_{ohm}
- Parasitic losses j_{leak}
- Exchange current density $j_{0, fu}^0, j_{0, ox}^0$
- Correction factor for concentration overpotential η_{conc}

Relative reactant depletion:

$$x_{i, dep} = \frac{x_{i, TPB}}{\sqrt{x_{i, in}}} \quad \text{Eq. (21)}$$

$$\eta_{conc, fu} = \eta_{conc, fu} C_{Fuel} \quad j > 0 \quad \text{Eq. (22)}$$

$$= \eta_{conc, fu} C_{Steam} \quad j < 0 \quad \text{Eq. (23)}$$

$$\eta_{conc, ox} = \eta_{conc, ox} C_{Air} \left(\frac{300}{\dot{V}_{air}} \right) \quad j > 0 \quad \text{Eq. (24)}$$

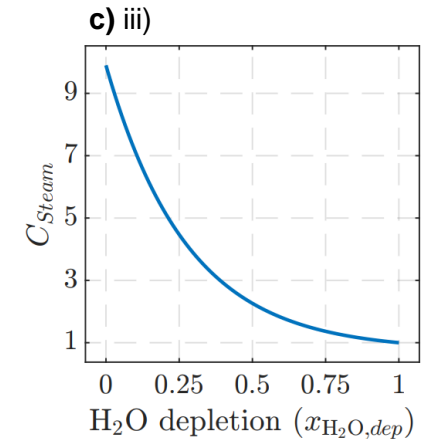
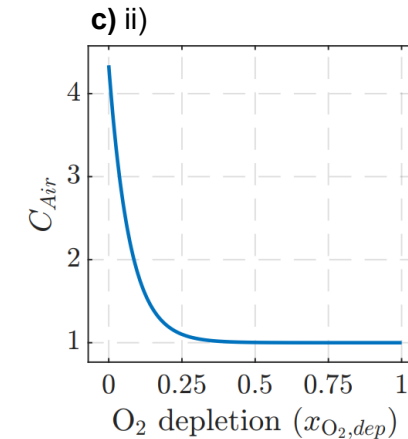
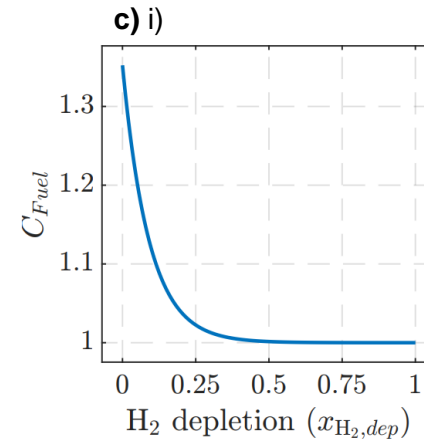
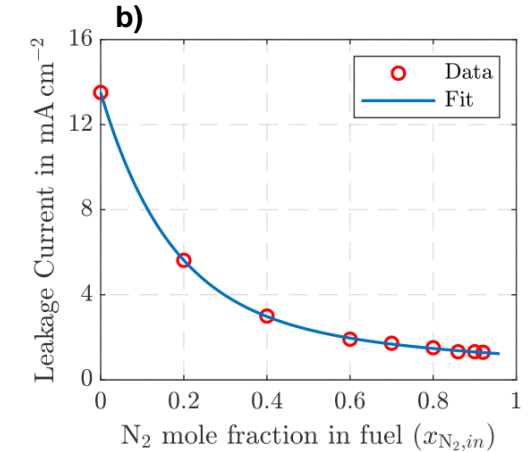
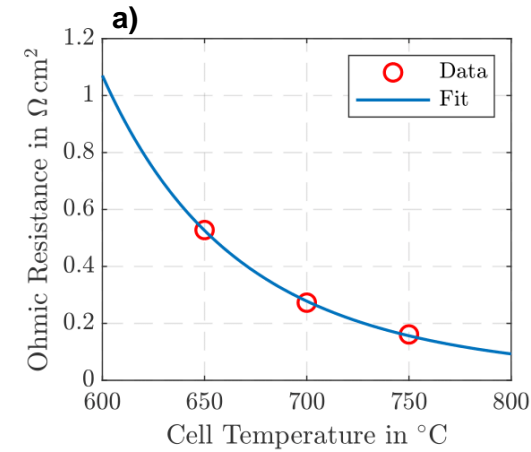


Fig.28: Fitting of a) ohmic resistance, b) parasitic losses, and c) correction factor for η_{conc} .